Electronic Supplementary Material (ESI) for ChemComm.

Supporting Information For

Selectively enhanced cancer therapy by marriage of metabolic alteration and mitochondria-targeted photodynamic therapy using cyclometalated Ir(III) complexes†

Jiangping Liu, [a] Chengzhi Jin, [a] Bo Yuan, [a] Xingguo Liu,[b] Yu Chen,[a] Liangnian Ji,[a] and Hui Chao*[a]

[a] MOE Key Laboratory of Bioinorganic and Synthetic Chemistry, School of Chemistry, Sun Yat-Sen University, Guangzhou 510275, China. E-mail: ceschh@mail.sysu.edu.cn, Fax: 86-20-84112245, Tel: 86-20-84110613

[b] Guangzhou Institute of Biomedicine and Health, Chinese Academy of Sciences, Guangzhou, 510530, China

Content

Materials

Unless otherwise noted, all chemical reagents and solvents were commercially available and used without further purification. Double distilled (DD) water was used throughout all of the experiments. $IrCl_3 \cdot xH_2O$, cisplatin, 2-phenylpyridine (ppy), 2,2-dichloroacetic anhydride, Ir standard solution (1000 μg/mL), 1,3-diphenyliso-benzofuran (DPBF), PBS, sodium pyruvate, 3-(4,5-dimethylthiazol-2-yl)-2,5-diphenyltetrazolium bromide (MTT), rhodamine B, agarose, 2',7'-dichlorofluorescin diacetate (DCFH-DA) and Lactate Colorimetric Assay Kit were purchased from Sigma-Aldrich and used without further purification. Dulbecco's modified eagle medium (DMEM), fetal bovine serum (FBS), penicillin, streptomycin and MitoTracker® Green FM were purchased from Invitrogen. JC-1 was purchased from Beyotime Biotechnology (China). Caspase-3/7 activity kit, CellTiter-Glo® 3D Cell Viability kit and CellTiter-Glo® Luminescent Cell Viability kit were purchased from Promega (USA). XF Cell Mito Stress Test Kit and XF Glycolysis Stress Test Kit were bought from Seahorse Bioscience. Nucleus extraction kit and cytoplasm extraction kit were purchased from Thermo pierce. The Ir(III) complexes were dissolved in DMSO preceding the experiments; the calculated quantities of the Ir(III) complexes solutions were then added to the appropriate medium to yield a final DMSO concentration of less than 0.2%. Cisplatin stock solution (3333 μM) were prepared by using normal saline solution, stored in the dark and used within 1 week.

Microananlysis (C, H and N) was performed using a Perkin-Elmer 240Q elemental analyzer. Electrospray ionization mass spectra (ES-MS) were recorded on a LCQ system (Finnigan MAT, USA). The ^1H NMR spectra were recorded on a Varian INOVA500NB Superconducting Fourier Transform Nuclear Magnetic Resonance Spectrometry. The UV-Vis spectra were recorded on a Varian Cary 300 spectrophotometer. Emission spectra were recorded on a PerkinElmer LS 55 fluorescence spectrometer at room temperature. Two-photon absorption cross section measurements were performed by a modelocked Ti: Sapphire laser (Coherent, USA) with a repetition rate of 80 MHz, and a femtosecond optical parametric amplifier (spectral tuning range 720–840 nm). Luminescence lifetime studies were performed with an Edinburgh FLSP-920 photo-counting system using a pulse laser (405 nm) as the excitation source. Luminescence quantum yields of iridium complexes in MeOH solution were measured with reference to $[Ru(bpy)_3]^{2+}$ (Φ_{PL} = 0.042, aerated MeOH, 25 °C)[1]. The inductively coupled plasma mass spectrometry (ICP-MS) experiments were carried out on an Agilent's 7700x instrument. Cell imaging was conducted on a LSM 710 (Carl Zeiss, Germany) Laser Scanning Confocal Microscope. Visible one-photon irradiation (λ_{irr} = 405 nm, 40 mW/cm^2) in PDT was provided by a commercially available LED visible area light source (Height LED Instruments, China). OCR and ECAR were determined by a Seahorse XF-24 extracellular flux analyzer (Seahorse Bioscience). ATP contents, caspase-3/7 contents were measured by an infinite M200 PRO equipment (TECAN, Swiss). All data were processed with the OriginPro 8.5 software package.

Synthesis and characterization

1,10-Phenanthroline-5,6-dione,[2] $[Ir(ppy)_2Cl]_2$[3] and **Ir4**[3] were synthesized according to the published methods. The synthetic routes of **Ir1-Ir3** were illustrated in Scheme S1. All of the final complexes were transferred into chloride salts with tetrabutylammonium chloride[2] for biological test.

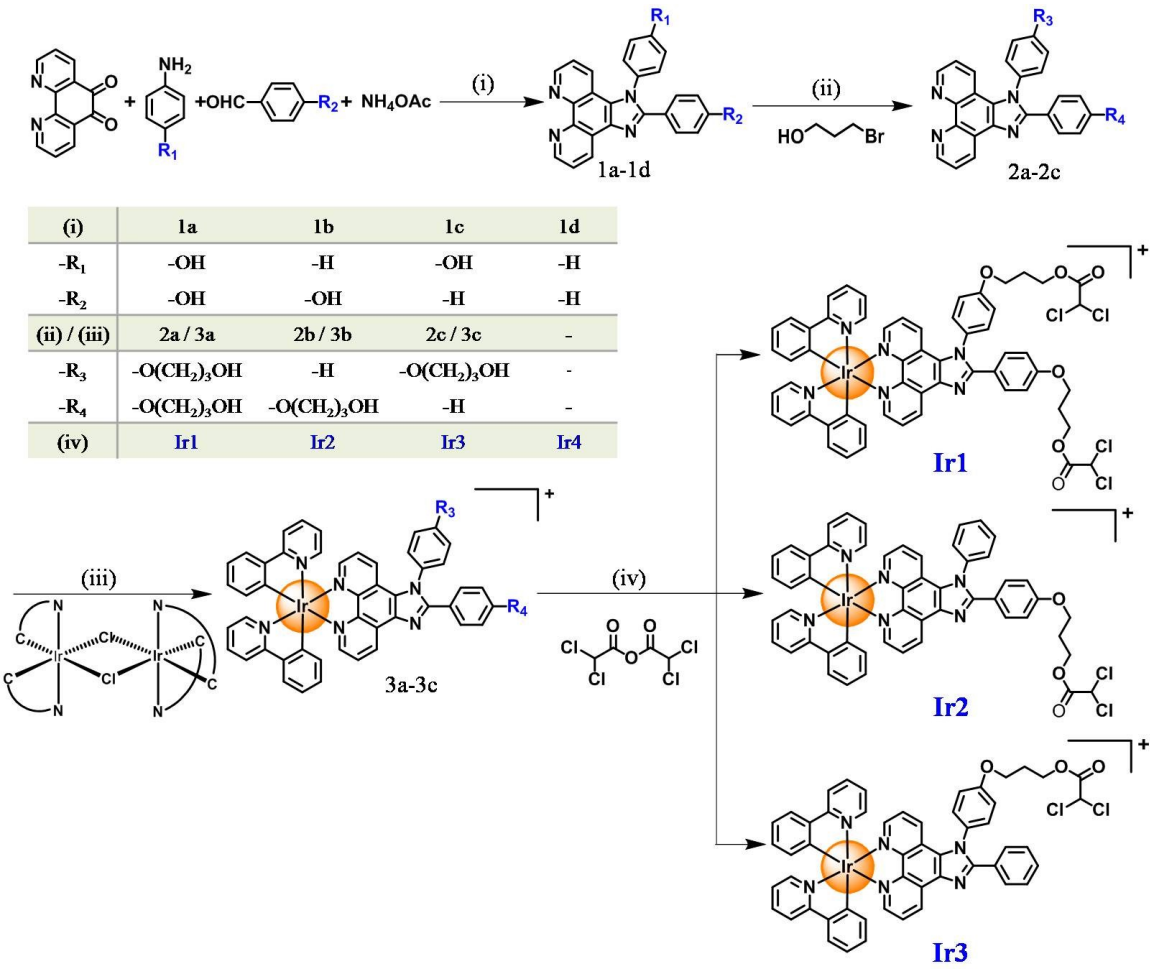

(i)	1a	1b	1c	1d
$-R_1$	-OH	-H	-OH	-H
$-R_2$	-OH	-OH	-H	-H
(ii) / (iii)	2a / 3a	2b / 3b	2c / 3c	-
$-R_3$	$-O(CH_2)_3OH$	-H	$-O(CH_2)_3OH$	-
$-R_4$	$-O(CH_2)_3OH$	$-O(CH_2)_3OH$	-H	-
(iv)	Ir1	Ir2	Ir3	Ir4

Scheme S1. Synthesis routes of **Ir1-Ir4**. (i) CH_3COOH, reflux overnight. (ii) DMF, K_2CO_3, Ar, reflux, 4 h. (iii) $CHCl_3$/MeOH, 65°C, 12 h. (iv) dry DCM, RT, 3 h.

Synthesis of 1a

A mixture of 4-hydroxybenzaldehyde (0.49 g, 4 mmol, 1 eqv.), ammonium acetate (3.7 g, 48 mmol, 12 eqv.), 1,10-Phenanthroline-5,6-dione (0.84 g, 4 mmol, 1 eqv.) and 4-aminophenol (0.48 g, 4.4 mmol, 1.1 eqv.) was dissolved in glacial acetic acid (40 mL), stirred under an argon atmosphere at 135 °C and allowed to reflux overnight. After cooling to room temperature, the solution was added with 50 mL water, adjusted to pH 6 using a 25% NH_3 solution. The precipitate was allowed to stand overnight at 4 °C and then filtered and dried under vacuum. The crude product was purified by silica gel chromatography using CH_2Cl_2/EtOH (20:1, v/v) as the eluent to afford a yellow product (Yield = 50.1%). Anal. Calcd. for C25H16N4O2 (%):C, 74.25; H, 3.99; N, 13.85. Found (%): C, 73.95; H, 4.01; N, 13.79. ES-MS: m/z = 405.05 [M+H]+. ^{1}H NMR (500 MHz, $CDCl_3$) δ 8.77 (ddd, J = 10.0, 7.5, 1.6 Hz, 2H), 8.51 (dd, J = 7.5, 1.4 Hz, 1H), 8.35 (dd, J = 7.5, 1.4 Hz, 1H), 7.93 (d, J = 7.5 Hz, 2H), 7.64 (t, J = 7.5 Hz, 1H), 7.59 (t, J = 7.5 Hz, 1H), 7.52 (d, J = 7.5 Hz, 2H), 6.98 (d, J = 7.5 Hz, 2H), 6.83 (d, J = 7.5 Hz, 2H), 6.24 (s, 1H), 5.68 (s, 1H).

Synthesis of 1b

The compound was synthesized by a similar method to 1a except that 4-aminophenol was replaced by aniline (Yield = 53.1%). Anal. Calcd. for C25H16N4O (%): C, 77.30; H, 4.15; N, 14.42. Found (%): C, 76.99; H, 4.17; N, 14.36. ES-MS: m/z = 389.05 [M+H]+. ^{1}H NMR (500 MHz, $CDCl_3$) δ 8.83 – 8.71 (m, 2H), 8.51 (dd, J = 7.5,

1.4 Hz, 1H), 8.37 (dd, J = 7.5, 1.4 Hz, 1H), 7.94 (d, J = 7.5 Hz, 2H), 7.64 (t, J = 7.5 Hz, 1H), 7.62 – 7.54 (m, 2H), 7.54 – 7.43 (m, 4H), 6.83 (d, J = 7.5 Hz, 2H), 5.70 (s, 1H).

Synthesis of 1c

The compound was synthesized by a similar method to 1a except that 4-hydroxybenzaldehyde was replaced by benzaldehyde (Yield = 51.8%). Anal. Calcd. for C25H16N4O (%): C, 77.30; H, 4.15; N, 14.42. Found (%): C, 76.97; H, 4.18; N, 14.34. ES-MS: m/z = 389.05 [M+H]+. ^{1}H NMR (500 MHz, $CDCl_3$) δ 8.77 (td, J = 7.6, 1.5 Hz, 2H), 8.51 (dd, J = 7.5, 1.6 Hz, 1H), 8.36 (dd, J = 7.5, 1.4 Hz, 1H), 8.16 – 8.06 (m, 2H), 7.64 (t, J = 7.5 Hz, 1H), 7.59 (t, J = 7.5 Hz, 1H), 7.52 (d, J = 7.5 Hz, 2H), 7.47 – 7.40 (m, 3H), 6.98 (d, J = 7.5 Hz, 2H), 6.24 (s, 1H).

Synthesis of 2a

A suspension of 1a (0.50 g, 1.24 mmol) and K_2CO_3 (0.43 g, 3.1 mmol) in DMF (10 mL) was stirred at ambient temperature for 30 min and then added with 3-bromopropan-1-ol (0.69 g, 5 mmol) and refluxed for 4 h. The reaction was monitored by TLC. Upon completion, the solution was concentrated, cooled to room temperature, added with ethyl acetate (50 mL) and washed with 2M KOH aqueous solution (2 × 20 mL). The organic layer was dried by Na_2SO_4 and evaporated under vacuum to afford a brownish crude mass. The product was obtained as a pale yellow powder by purification with silica gel chromatography using CH_2Cl_2/EtOH (25:1, v/v) as the eluent (Yield = 85.2%). Anal. Calcd. for C31H28N4O4 (%):C, 71.52; H, 5.42; N, 10.76. Found (%): C, 71.16; H, 5.45; N, 10.71. ES-MS: m/z = 521.05 [M+H]+. ^{1}H NMR (500 MHz, $CDCl_3$) δ 8.77 (ddd, J = 10.0, 7.5, 1.4 Hz, 2H), 8.51 (dd, J = 7.5, 1.4 Hz, 1H), 8.36 (dd, J = 7.5, 1.4 Hz, 1H), 8.07 (d, J = 7.5 Hz, 2H), 7.63 (m, 4H), 6.98 (dd, J = 7.3, 5.7 Hz, 4H), 4.84 (s, 1H), 4.86 (s, 1H), 4.27 (t, J = 5.3 Hz, 2H), 4.19 (t, J = 7.7 Hz, 2H), 3.86 – 3.64 (m, 4H), 2.15 – 1.98 (m, 4H).

Synthesis of 2b

The compound was synthesized by a similar method to 2a (Yield = 83.6%). Anal. Calcd. for C28H22N4O2 (%): C, 75.32; H, 4.97; N, 12.55. Found (%): C, 74.87; H, 4.99; N, 12.47. ES-MS: m/z = 447.15 [M+H]+. ^{1}H NMR (500 MHz, $CDCl_3$) δ 8.91 (dd, J = 7.5, 1.4 Hz, 2H), 8.56 (dd, J = 7.5, 1.4 Hz, 1H), 8.46 (dd, J = 7.5, 1.6 Hz, 1H), 8.08 (d, J = 7.5 Hz, 2H), 7.65 (dt, J = 15.1, 7.5 Hz, 2H), 7.55 (ddd, J = 8.9, 6.0, 2.5 Hz, 1H), 7.50 – 7.40 (m, 4H), 6.98 (d, J = 7.5 Hz, 2H), 4.23 (t, J = 4.9 Hz, 2H), 3.78 (t, J = 7.6 Hz, 2H), 2.86 (s, 1H), 2.05 (tt, J = 7.6, 4.9 Hz, 2H).

Synthesis of 2c

The compound was synthesized by a similar method to 2a (Yield = 88.4%). Anal. Calcd. for C28H22N4O2 (%): C, 75.32; H, 4.97; N, 12.55. Found (%): C, 74.96; H, 4.98; N, 12.46. ES-MS: m/z = 447.05 [M+H]+. ^{1}H NMR (500 MHz, $CDCl_3$) δ 8.77 (ddd, J = 7.6, 6.6, 1.4 Hz, 2H), 8.51 (dd, J = 7.4, 1.5 Hz, 1H), 8.35 (dd, J = 7.5, 1.4 Hz, 1H), 8.19 – 8.05 (m, 2H), 7.73 – 7.63 (m, 3H), 7.59 (t, J = 7.5 Hz, 1H), 7.50 – 7.36 (m, 3H), 6.97 (d, J = 7.5 Hz, 2H), 4.27 (t, J = 4.8 Hz, 2H), 3.80 (t, J = 7.8 Hz, 2H), 2.96 (s, 1H), 2.06 (tt, J = 7.8, 4.8 Hz, 2H).

Synthesis of 3a

A mixture of $[Ir(ppy)_2Cl]_2$ (0.25 g, 0.233 mmol) and 2a (0.215 g, 0.414 mmol) was protected from light and refluxed under argon in $CH_3OH/CHCl_3$ (15 ml/30 mL) binary solution for 8 h. Upon completion, the solution was evaporated. The resultant solid was purified by column chromatography on alumina with CH_2Cl_2/EtOH to afford the pure product (Yield = 68.1%). Anal. Calcd. for C53H44ClIrN6O4 (%): C, 60.25; H, 4.20; N, 7.95. Found (%): C, 60.01; H, 4.22; N, 7.91. ES-MS: m/z = 1021.05 [M-Cl]+. ^{1}H NMR (500 MHz, d6-DMSO) δ 9.30

(d, J = 9.0 Hz, 1H), 8.27 (dd, J = 14.3, 8.3 Hz, 2H), 8.23 (d, J = 4.9 Hz, 1H), 8.14 (dd, J = 8.2, 5.1 Hz, 1H), 8.08 (d, J = 4.6 Hz, 1H), 7.96 (dd, J = 13.8, 7.9 Hz, 2H), 7.89 (q, J = 7.3 Hz, 2H), 7.79 (dd, J = 8.6, 5.1 Hz, 1H), 7.69 (d, J = 9.0 Hz, 2H), 7.59 (dd, J = 8.1, 6.1 Hz, 3H), 7.48 (d, J = 5.7 Hz, 2H), 7.25 (dd, J = 14.2, 8.3 Hz, 2H), 7.11 – 6.87 (m, 8H), 6.28 (dd, J = 14.3, 7.5 Hz, 2H), 4.84 (s, 1H), 4.86 (s, 1H), 4.47 (t, J = 6.3 Hz, 2H), 4.40 (t, J = 6.3 Hz, 2H), 4.20 (t, J = 6.0 Hz, 2H), 4.09 (t, J = 6.1 Hz, 2H), 2.26 – 2.16 (m, 2H), 2.16 – 2.05 (m, 2H).

Synthesis of 3b

The compound was synthesized by a similar method to 3a (Yield = 66.4%). Anal. Calcd. for C50H38ClIrN6O2 (%): C, 61.12; H, 3.90; N, 8.55. Found (%): C, 60.87; H, 3.92; N, 8.51. ES-MS: m/z = 947.20 [M-Cl]+. ^{1}H NMR (500 MHz, d6-DMSO) δ 9.32 (dd, J = 8.3, 1.4 Hz, 1H), 8.33 – 8.21 (m, 3H), 8.16 (dd, J = 8.4, 5.1 Hz, 1H), 8.10 – 8.05 (m, 1H), 7.97 (d, J = 7.2 Hz, 1H), 7.94 (d, J = 7.4 Hz, 1H), 7.92 – 7.86 (m, 2H), 7.82 – 7.70 (m, 6H), 7.56 (d, J = 8.9 Hz, 2H), 7.48 (dd, J = 11.7, 3.5 Hz, 3H), 7.10 – 6.92 (m, 8H), 6.28 (dd, J = 16.5, 7.3 Hz, 2H), 4.86 (s, 1H), 4.42 (t, J = 6.3 Hz, 2H), 4.06 (t, J = 6.2 Hz, 2H), 2.08 (p, J = 6.2 Hz, 2H).

Synthesis of 3c

The compound was synthesized by a similar method to 3a (Yield = 70.4%). Anal. Calcd. for C50H38ClIrN6O2 (%): C, 61.12; H, 3.90; N, 8.55. Found (%): C, 60.90; H, 3.92; N, 8.50. ES-MS: m/z = 947.20 [M-Cl]+. ^{1}H NMR (500 MHz, d6-DMSO) δ 9.30 (dd, J = 8.4, 1.4 Hz, 1H), 8.25(ddd, J = 9.6, 6.5, 4.9 Hz, 3H), 8.14 (dd, J = 8.3, 5.1 Hz, 1H), 8.10 (dd, J = 5.1, 1.2 Hz, 1H), 7.96 (dd, J = 14.0, 7.9 Hz, 2H), 7.88 (td, J = 8.4, 1.3 Hz, 2H), 7.80 (dd, J = 8.6, 5.1 Hz, 1H), 7.70 (d, J = 9.1 Hz, 2H), 7.67 – 7.60 (m, 3H), 7.51 – 7.41 (m, 5H), 7.29 – 7.20 (m, 2H), 7.11 – 6.91 (m, 6H), 6.29 (dd, J = 14.2, 7.3 Hz, 2H), 4.88 (s, 1H), 4.48 (t, J = 6.3 Hz, 2H), 4.22 (t, J = 6.1 Hz, 2H), 2.25 – 2.10 (m, 2H).

Synthesis of **Ir1**

A solution of 3a (0.28 g, 0.27 mmol, 1eqv.) in dry CH_2Cl_2 (35 mL) was prepared in round-bottom flask and purged with argon. Dichloroacetate anhydride (0.32 g, 1.3 mmol, 5eqv.) was added dropwise to the solution. The reaction was stirred at room temperature for 5 h. Upon completion, the solvent was evaporated to dryness to give an orange solid which was then dissolved in aqueous methanol. The chloride salt was converted into the hexafluorophosphate salts by anion metathesis with aqueous NH_4PF_6; the precipitates were collected, washed with adequate water and dried under vacuum. Further purification was conducted by recrystalizaiont with toluene/$CHCl_3$ (Yield = 78%). Anal. Calcd. for C57H44Cl4F6IrN6O6P (%):C, 49.32; H, 3.20; N, 6.05. Found (%): C, 49.07; H, 3.21; N, 6.02. ES-MS: m/z = 1243.20 [M-PF6]+. ^{1}H NMR (500 MHz, d6-DMSO) δ 9.30 (d, J = 9.0 Hz, 1H), 8.27 (dd, J = 14.3, 8.3 Hz, 2H), 8.23 (d, J = 4.9 Hz, 1H), 8.14 (dd, J = 8.2, 5.1 Hz, 1H), 8.08 (d, J = 4.6 Hz, 1H), 7.96 (dd, J = 13.8, 7.9 Hz, 2H), 7.89 (q, J = 7.3 Hz, 2H), 7.79 (dd, J = 8.6, 5.1 Hz, 1H), 7.69 (d, J = 9.0 Hz, 2H), 7.59 (dd, J = 8.1, 6.1 Hz, 3H), 7.48 (d, J = 5.7 Hz, 2H), 7.25 (dd, J = 14.2, 8.3 Hz, 2H), 7.11 – 6.87 (m, 10H), 6.28 (dd, J = 14.3, 7.5 Hz, 2H), 4.47 (t, J = 6.3 Hz, 2H), 4.40 (t, J = 6.3 Hz, 2H), 4.20 (t, J = 6.0 Hz, 2H), 4.09 (t, J = 6.1 Hz, 2H), 2.26 – 2.16 (m, 2H), 2.16 – 2.05 (m, 2H).

Synthesis of **Ir2**

The compound was synthesized by a similar method to Ir1 (Yield = 74 %). Anal. Calcd. for C52H38Cl2F6IrN6O3P (%): C, 51.92; H, 3.18; N, 6.99. Found (%): C, 51.66; H, 3.20; N, 6.96. ES-MS: m/z = 1057.10 [M-PF6]+. ^{1}H NMR (500 MHz, d6-DMSO) δ 9.32 (dd, J = 8.3, 1.4 Hz, 1H), 8.33 – 8.21 (m, 3H), 8.15 (dd, J = 8.3, 5.1 Hz, 1H), 8.10 – 8.05 (m, 1H), 7.97 (d, J = 7.2 Hz, 1H), 7.94 (d, J = 7.4 Hz, 1H), 7.92 – 7.86

(m, 2H), 7.82 – 7.70 (m, 6H), 7.56 (d, J = 8.9 Hz, 2H), 7.48 (dd, J = 11.7, 3.5 Hz, 3H), 7.10 – 6.92 (m, 8H), 6.89 (s, 1H), 6.28 (dd, J = 16.5, 7.3 Hz, 2H), 4.40 (t, J = 6.3 Hz, 2H), 4.08 (t, J = 6.1 Hz, 2H), 2.10 (p, J = 6.2 Hz, 2H).

Synthesis of **Ir3**

The compound was synthesized by a similar method to Ir1 (Yield = 77%). Anal. Calcd. for C52H38Cl2F6IrN6O3P (%):C, 51.92; H, 3.18; N, 6.99. Found (%): C, 51.69; H, 3.19; N, 6.97. ES-MS: m/z = 1057.10 [M-PF6]+. ^{1}H NMR (500 MHz, d6-DMSO) δ 9.32 (dd, J = 8.3, 1.4 Hz, 1H), 8.25 (ddd, J = 9.6, 6.5, 4.9 Hz, 3H), 8.15 (dd, J = 8.3, 5.1 Hz, 1H), 8.10 (dd, J = 5.1, 1.2 Hz, 1H), 7.96 (dd, J = 14.0, 7.9 Hz, 2H), 7.89 (td, J = 8.6, 1.3 Hz, 2H), 7.81 (dd, J = 8.6, 5.1 Hz, 1H), 7.70 (d, J = 9.1 Hz, 2H), 7.67 – 7.60 (m, 3H), 7.51 – 7.41 (m, 5H), 7.29 – 7.20 (m, 2H), 7.11 – 6.91 (m, 7H), 6.29 (dd, J = 14.2, 7.3 Hz, 2H), 4.47 (t, J = 6.3 Hz, 2H), 4.20 (t, J = 6.1 Hz, 2H), 2.26 – 2.13 (m, 2H).

Two-photon cross section determination

The two-photon cross sections were determined over a broad spectral region (720-840 nm) by the matured TPEF method devised by Webb and Xu[4] relative to Rhodamine B in methanol as standard.[5] The two-photon induced fluorescence was excited by a modelocked Ti:Sapphire laser with a repetition rate of 80 MHz (laser pulse = 100 fs) combined with a femtosecond optical parametric amplifier and the data were acquired by a charge-coupled device (CCD). The quadratic dependence of two-photon induced fluorescence intensity on the excitation power was validated at the wavelength where the corresponding two-photon cross section reached maximum. The two-photon cross section of **Ir1-Ir4** can be calculated by the following equation,

$$\sigma_S = \sigma_R \frac{\phi_R C_R I_S n_S}{\phi_S C_S I_R n_R} \quad (1)$$

where *I* is the integrated fluorescence intensity, *Φ* stands for fluorescence quantum yield, *σ* denotes the two-photon cross sections, *C* represents the concentration of **Ir1-Ir4**, and *n* is the refractive index. Subscript "*S*" stands for sample and "*R*" stands for reference, i.e. Rhodamine B.

Singlet oxygen detection in solution

The photosensitizing ability was assessed by direct and indirect methods. The direct verification of singlet oxygen is to observe the 1273 nm[6] phosphorescence of singlet oxygen provoked by **Ir1-Ir4** (OD_{405nm} = 0.2) in $CDCl_3$ in the presence of light (405 nm). For the indirect method, DPBF was adopted as the singlet oxygen scavenger of which the absorbance at 479 nm declined as the singlet oxygen generated. Specifically, a mixture of DPBF (30 μM) and the indicated compounds with adjusted concentration (OD_{405nm} = 0.2) were exposed to irradiation (405 ± 10 nm, 20 mW cm^{-2}) and the emission intensity at 479 nm was recorded every 5 second. $[Ru(bpy)_3]^{2+}$ was utilized as the standard (Φ_Δ= 0.81 in methanol[7]). The slopes derived from linear regression of the plots of Δ[DPBF] versus time were used to calculate the singlet oxygen quantum yields of **Ir1-Ir4** which were finally determined by the following formulas[8]:

$$-\frac{\Delta[DPBF]}{t} = \frac{I_0 - I_t}{t} = I_{in}\Phi_{ab}\Phi_\Delta\Phi_r \quad (2)$$

$$\frac{S}{S^r} = \frac{\Phi_{ab}}{\Phi_{ab}^r}\frac{\Phi_\Delta}{\Phi_\Delta^r} \quad \text{.....(3)}$$

where I_{in} denotes the incident monochromatic light intensity, Φ_{ab} represents the light absorbing efficiency at 405 nm, Φ_r stands for the reaction quantum yield of DPBF, Φ_Δ is the singlet oxygen quantum yield, t is the cumulative radiation time, I_0/I_t is the fluorescence intensity before/after irradiation of the complexes, and S is the slope of plots. The superscript r indicates the reference.

Electron spin resonance (ESR) measurements

The ESR spectra were recorded at room temperature (25 °C) on a Bruker Model A300 spectrometer at 1 G field modulation and 100 G scan range with 20 mW microwave power. An area light source was used for irradiation for 5 min (405 ± 10 nm, 20 mW cm^{-2}). **Ir1-Ir4** (OD_{405nm} = 0.2) were dissolved in aerated methanol containing 10 mM TEMP as a $^1O_2$ spin trap and sucked into capillary tubes by siphon effect in the dark, respectively. The loaded capillary tubes were sintered at one terminal, subjected to irradiation and subsequently the measurement was carried out to plot the ESR spectra of the reaction product. The control group was set to be methanol solution containing solo TEMP.

Cell line and culture

HeLa, L02, A549, A549R cells were obtained from the American Type Culture Collection (ATCC, Manassas, VA). The cell lines were maintained in DMEM media supplemented with fetal bovine serum (10%), penicillin (100 units/mL) and streptomycin (50 units/mL) at 37 °C in a CO_2 incubator (95% relative humidity, 5% CO_2).

Intracellular distribution studies

The intracellular distribution study comprises of two sections, co-localization study by confocal laser scanning microscopy (CLSM) and ICP-MS. For confocal study, HeLa cells were seeded onto 35 mm Corning confocal dishes at a density of 1 × 10^4 cells/mL and allowed to adhere overnight. After incubation with 50 nM MitoTracker® Green for 30 min at 37 °C, the cells were washed with PBS and continued to incubate with 0.2 μM **Ir1-Ir4** complexes for 1 h in the dark, respectively at 37 °C. Upon completion, the cells were washed by PBS for three times and subjectd to confocal microscopy. For the MitoTracker Green channel, the dye was excited at 488 nm, and the emission filter was between 505-525 nm. For the Ir channel, the one-photon excitation wavelenth was 405 nm, and the emission signals were collected between 560-640 nm. For two-photon channel, Ir was excited at the wavelength corresponding to the maximum two-photon cross section of each Ir complex.

For ICP-MS study, exponentially growing HeLa cells were treated with **Ir1-Ir4** under identical conditions, respectively. Upon completion of the incubation the cells were trypsinized, collected and counted. The cells were devided into two equal parts and processed with nucleus extraction kit and cytoplasm extraction kit by the manufacturer's protocol, repectively. The extrations were subsequently digested by 60% HNO_3 for over 24 h, and diluted by DD water to obtain 2% HNO_3 sample solutions for final determination. The Ir content was determined by standard curve method, and the content in nuclei, mitochondria and the whole cell was calculated associated with the cell numbers.

Ir(III) internalization mechanism study

The internalization mechanism study was conducted by CLSM.[9] HeLa cells adherent to confocal dishes at a density of 1 × 10^4 cells/mL were treated with various combination of compounds in different conditions. Specifically, for temperature dependent uptake study, HeLa cells were treated with 0.2 μM **Ir1** for 1 h at 4 °C, 20 °C and 37 °C, respectively. For bio-inhibiting uptake study, 2-deoxygen-D-glucose (2-dG, 50 mM) and oligomycin (5 μM) were utilized as energy blocker to inhibit active transport. HeLa cells were pretreated with 2-dG and oligomycin in special culture medium without glucose at 37 °C for 45 min and further treated with 0.2 μM **Ir1** for 1 h in the dark. NH_4Cl (50 mM) and chloroquine (100 μM) were used to inhibit endocytotic uptake. HeLa cells pretreated with the indicated endocytotic inhibitors at 37 °C for 1 h were treated with 0.2 μM **Ir1** for 1 h in the dark. All of the HeLa cells were washed with PBS for 3 times and subjected to CLSM. The Ir channel was set to be identical to that of co-localization study.

Mitochondrial membrane potential (MMP) assessment

MMP was assessed by JC-1 staining. HeLa/L02 cells were seeded onto Corning confocal dishes at a density of 1 × 10^4 cells/mL and allowed to adhere overnight. The cells were treated with culture medium (control), 20 μM DCA, and 0.5 μM **Ir1-Ir4**, respectively, for 6 h in the dark and then washed with PBS. Then the cells were cultured with JC-1 (10 μg/mL) in PBS for 20 min in the dark. The fluorescent images were captured by CLSM. The excitation wavelength for JC-1 monomer was 488 nm, and the emission filter was adjusted to around 529 nm for JC-1 monomer (green). As for JC-1 aggregate channel, the excitation was 543 nm, and the emission were collected around 590 nm (red).

Caspase-3/7 activation detection assay

HeLa/L02 cells were seeded in white-walled nontransparent-bottomed 96-well micro-culture plates at a density of 1.5 × 10^4 cells/well and allowed to incubated overnight to adhere. The cells were then treated with culture medium, 20 μM cisplatin, 20 μM DCA, 0.5 μM **Ir1-Ir4**, respectively. The cells were incubated for 10 h in the dark and divided into two equal parts. Dark group was incubated for additional 2 h and treated with Caspase-3/7 activity kit according to the manufacturer's protocol and the luminescence in RLUs was quantified by an Infinite M200 PRO (TECAN, Swiss). The other was exposed to LED area light irradiation (405 ± 10 nm, 6 J cm^{-2}), and incubated for additional 2 h in the dark. The caspase-3/7 activity was measured by identical method.

HeLa cell metabolism test

The mitochondrial OXPHOS and glycolysis function of HeLa cells was measured by determining the oxygen consumption rate (OCR) and extracellular acidification rate (ECAR) with a Seahorse XF24 extracellular flux analyzer. HeLa cells were seeded at a density of 5 × 10^4 cells/well to the XF24-well culture microplates (Seahorse Bioscience) the day before Seahorse test. The sensor cartridge was hydrated by being immersed in calibration buffer at 37 °C in non-CO_2 incubator overnight. For measuring OCR, the assay medium was consist of sodium pyruvate (2 mM), glucose (25 mM) and L-glutamine (2 mM) in unbuffered DMEM. For glycolysis test, the assay medium was consist of L-glutamine (4 mM) in unbuffered DMEM. The as-prepared

culture medium was adjusted to pH 7.4, sterilized and stored at 4 °C. HeLa cells were treated with 0.5 μM **Ir1-Ir4**, 20 μM DCA, respectively, for 2 h in the dark. For the light group, the cells were subsequently exposed to LED area light source (405 ± 10 nm, 6 J cm^{-2}) while the dark group stay unchanged. Both groups were incubated for another 2 h in the dark and the cell metabolism were assessed including OCR and ECAR by using XF Cell Mito Stress Test Kit and XF Glycolysis Stress Test Kit, respectively, according to the manufacturer's protocols. OCR and ECAR levels were recorded by the sensor cartridge and the measured values were calibrated based on the cell viability tested in viability assay. Different OXPHOS parameters were calculated by subtracting the average respiration rates before and after the injection of electron transport inhibitor (oligomycin A, 1 μM), the electron chain transport (ETC) accelerator (FCCP, 500 nM), and a mixture of complex III inhibitor (antimycin A, 1 μM) and complex I inhibitor (rotenone, 1 μM). The parameters calculated include: non-mitochondrial respiration (respiration after antimycin A/rotenone injection), basal respiration (baseline respiration minus non-mitochondrial respiration), maximal respiratory capacity (respiration stimulated by FCCP minus non-mitochondrial respiration), and spared respiratory capacity (maximal respiration minus basal respiration). Different glycolytic parameters were also calculated by subtracting the average acidification rates before and after the injection of glycolysis substrate (glucose, 10 mM), electron transport inhibitor (oligomycin A, 1 μM), and glycolysis inhibitor (2-dG, 50 mM). The glycolytic parameters were calculated including: non-glycolytic acidification (average acidification after 2-dG injection), glycolysis (post glucose injection acidification minus non-glycolytic acidification), glycolytic capacity (post oligomycin A injection acidification minus non-glycolytic acidification), and glycolytic reserve (glycolytic capacity minus glycolysis). All test results had two replicates.

Lactate concentration measurement

Lactate concentration measurement was carried out by enzymatic assays using Lactate Colorimetrci Assay Kit (Sigma-Aldrich). HeLa cells were seeded onto 6-well culture plates at a concentration of 2 × 10^6 cells/well. After attachment, the cells were treated with culture medium, 20 μM DCA, 0.5 μM **Ir1-Ir4**, respectively, for 2 h in the dark. Then the light group was exposed to light irradiation (405 ± 10 nm, 6 J cm^{-2}) while the dark group remained unchanged. Both groups were further incubated for 2 h. The media were removed and the cells were rapidly homogenized in ice-cold buffer. The cell lysate were centrifuged and the supernatant fluid was processed with the enzyme mix and substrate working reagent. The mixture was allowed to incubate in the dark for 30 min at room temperature. Upon completion, the samples were vigorously vibrated and the absorption at 450 nm was measured. The lactate level in cells (ng per cell) was determined in association with cell numbers and lactate standard curve.

ATP quantification

HeLa cells were seeded on white-walled nontrasparent-bottomed 96-well micro-culture plates at a density of 1.5 × 10^4 cells/well and allowed to incubate overnight to adhere. The cells were treated with culture medium, 20 μM DCA, 0.5 μM **Ir1-Ir4**, respectively, for 2 h in the dark. Then the light group was exposed to light irradiation (405 ± 10 nm, 6 J cm^{-2}) while the dark group remained unchanged. Both groups were further incubated for 2 h. Upon completion, each well was added equal volume of CellTiter-Glo® Luminescent Cell

Viability kit (Promega) and vigourously vibrated. The chemoluminescence were measured by a TECAN Infinite M200 PRO multifunctional reader. The net ATP induced luminescence intensity in each weill was obtained after subtracting that of blank wells. Luminescence intensity in control wells were set to be 100%. Relative ATP contents of other groups were presented by their luminescence intensity ratios to control group.

3D multicellular spheroids (MCSs) formation and analysis

The MCSs were prepared by a similar method to our previous report.[2] Briefly, 1% agarose in DMEM was sterilized and injected to 96-well micro-assay culture plates (50 μL/well). The plates were then exposed to UV irradiation for 3 h and added with 200 μL/well HeLa sigle-cell suspension (1 × 10^4 cells/mL). MCSs formed spontaneously 2-3 days afterwards with diamerter around 400 μm. After the formation of MCSs, the integrity of MCSs were examined and the diameters were measured by a phase contrast inverted microscope using a 10× objective (Zeiss Axio Observer D1, Germany). The volume of MCS was calculated by the equation[10]:

$$Volume = \frac{4}{3}\pi r^3 \quad \cdots\cdots (4)$$

Z-stack imaging of 3D MCSs

3D MCSs pretreated with 0.2 μM **Ir1-Ir4** for 2 h, respectively, in the dark were carefully washed by PBS and subjected to CLSM for scanning. The one-/two-photon excited luminescence along the z axis were collected and processed. The images were stacked in the z-stack mode to give a final one-/two-photon z-axis stack imaging.

Two-photon induced singlet oxygen generation *in vitro*

Singlet oxygen generation was verified in both monolayer cells and MCSs by using DCFH-DA as the singlet oxygen probe.[11] For monolayer model, adherent HeLa cells were pretreated with 0.5 μM **Ir1-Ir4** at 37 °C for 1 h, respectively and then incubated with PBS containing 10 μM DCFH-DA at room temperature for 20 min. The culture medium was refreshed with fresh PBS and exposed to two-photon laser irradiation (10 s, 1.2 W cm^{-2}, 1kHz, pulse width 110 fs) at the wavelength corresponding to their maximum TPA cross sections. The fluorescent images were captured by an LSM 710 Carl Zeiss Laser Scanning Confocal Microscopy. For the DCFH-DA channel, the excitation wavelength was 488 nm and the emission filter was between 510-550 nm. For 3D model, MCSs were incubated with Ir complex and DCFH-DA successively for a doubled time span at 37 °C and subjected to two-photon laser irradiation (10 s/section, section interval = 3 μm, 1.2 W cm^{-2}, 1kHz, pulse width 110 fs). The MCSs were imaged by identical operation with monolayer cells.

Long-term growth inhibition and visualization of live/dead cells within MCSs

MCSs were incubated with culture medium, 20 μM cisplatin, 20 μM DCA, 0.5 μM **Ir1-Ir4**, a combination of 0.5 μM **Ir4** with 0.5 μM DCA, and a combination of 0.5 μM **Ir4** with 1 μM DCA, respectively, for 12 h and then the culture medium were refreshed and incubated for 3 days in the dark. Then the MCSs were exposed to two-photon laser irradiation (1.2 W cm^{-2}, 1kHz, pulse width 110 fs, light dose = 12 J cm^{-2} per section, interval = 3 μm) at 730 nm (control, cisplatin, DCA, **Ir2**, **Ir3**)/740 nm (**Ir1**)/750 nm (**Ir4**) and the samples were incubated in

the dark for additional 3 days. The 50% culture media exchange was performed every 48 h in this duration. The images of the MCSs were captured by an inverted microscope (Ziess Axio Observer D1, Germany) everyday and the volumes of MCSs were calculated and plotted over 6 days. The visualization of live/dead assay of MCSs was performed by using the Viability/Cytotoxicity Kit for mammalian cells (Life Technologies). The viable/dead cells of as-treated MCSs before two-photon laser irradiation (day 3) and 48 h after TP-PDT (day 5) were visualized by calcein AM and EthD-1. The MCSs were incubated with 2 μM calcein AM and 4 μM EthD-1 in culture medium for 45 min and imaged directly using an inverted fluorescence microscope (Ziess Axio Observer D1, Germany). Calcein AM can distinguish live cells by reacting with the ubiquitous esterases in living cells to yield a green fluorescent product (λ_{ex}=495 nm, λ_{em}=515 nm). While EthD-1 can penetrate damaged membrane to access nucleic acids to recover red fluorescence (λ_{ex}=495 nm, λ_{em}=635 nm). The ratio of green/red fluorescence can therefore reflect the live/dead cell ratio within MCSs.

Evaluation of (photo)toxicity

(Photo)cytotoxicity of **Ir1-Ir4** complexes in both monolayer cells and 3D MCSs were tested. H_2TPP was utilized as the positive control. For monolayer cell viability test, exponentially grown HeLa/L02/A549/A549R cells were seeded in triplicate into white-walled non-transparent bottomed 96-well plates at 1 × 10^4 cells/well and incubated for 24 h to adhere. Then the cells were treated with increasing concentration of the tested compounds (control, H_2TPP, cisplatin, DCA, **Ir1-Ir4**) and combination of compouds (DCA+**Ir4**, mol ratio 1:1 and 1:2, respectively). Control wells were treated with solo culture medium. Blank group contained only culture medium without any cells. All groups were incubated for 12 h, and then the culture medium were refreshed and cells were incubated for another 12 h. Upon completion, for the light group, the cells were subjected to OP irradiation (405 ± 10 nm, 20 mW cm^{-2}, light dose = 6 J cm^{-2}). While for the dark group, the cells were kept in the dark. All groups were further incubated for 48 h and treated with CellTitler-Glo® Luminescent Cell Viability kit (Promega) and the chemolumenescence was measured by an Infinite M200 PRO (TECAN) multifunctional reader. The cell survival rate in control wells were considered to be 100%, all data were subtrated to blank value before calculating the survival rate. IC_{50} values were determined by plotting the percentage of viability versus concentration on a logarithmic graph.

For 3D models, the HeLa MCSs cultured by the afore mentioned method were carefully transferred to white-walled non-transparent bottomed 96-well plates (1 spheroid per well). And the MCSs were devided and received PDT treatment regimen in a similar way except that the light group of MCSs was futher devided into two equal parts which received distinct irradiation condition. In detail, for OP irradiation group, MCSs were irradiated by area light source (405 ± 10 nm, 20 mW cm^{-2}, light dose = 12 J cm^{-2}), for TP irradiation group, MCSs were irradiated by pulzed laser at 730 nm (control, H_2TPP, cisplatin, DCA, **Ir2**, **Ir3**)/740 nm (**Ir1**)/750 nm (**Ir4**) (1.2 W cm^{-2}, light dose = 12 J cm^{-2}). All groups were ultimated treated with CellTitler-Glo® 3D Cell Viability kit (promega) and the results were processed by an identical method.

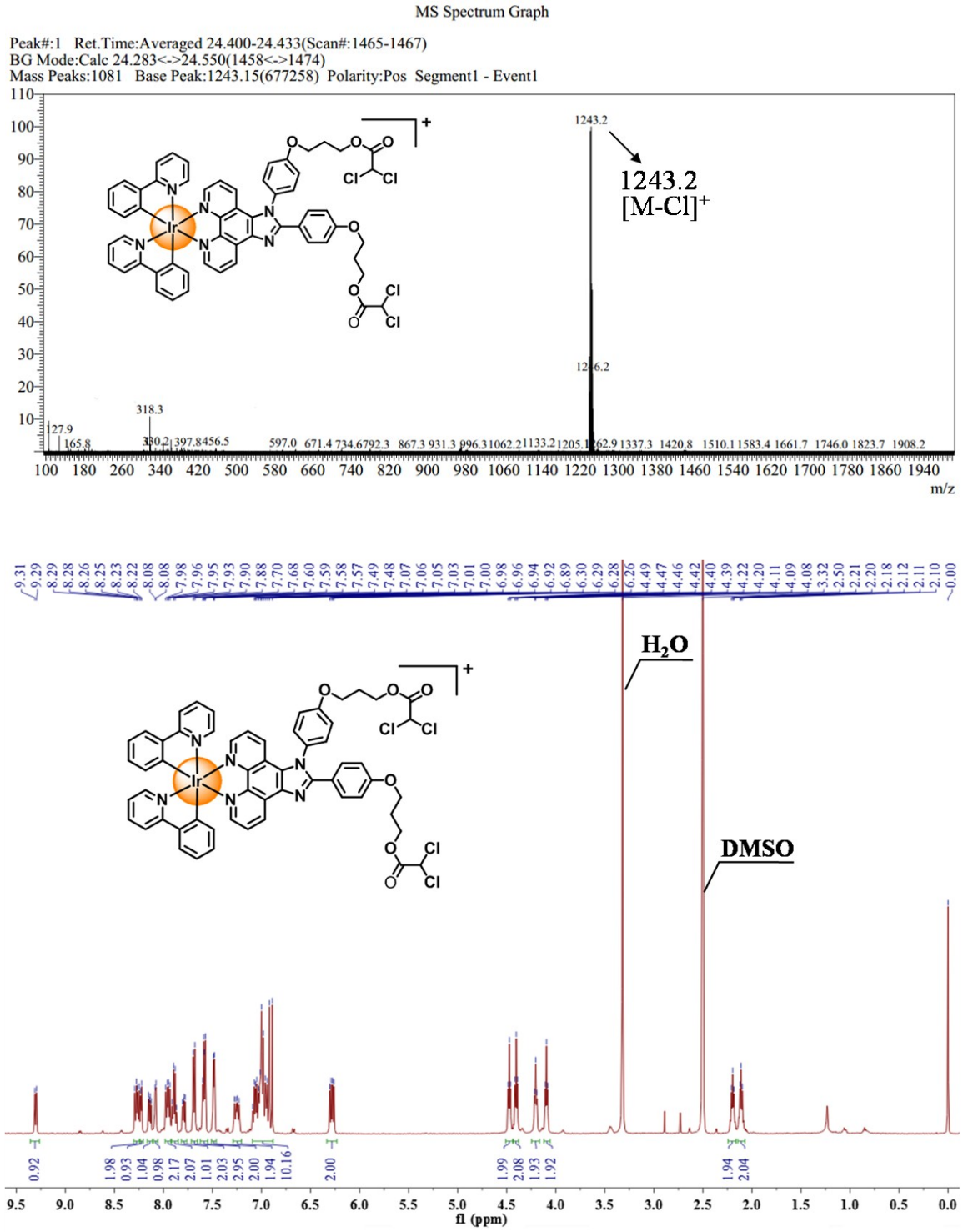

Figure S1. ESI-MS, and ^{1}H NMR spectrum of **Ir1**。

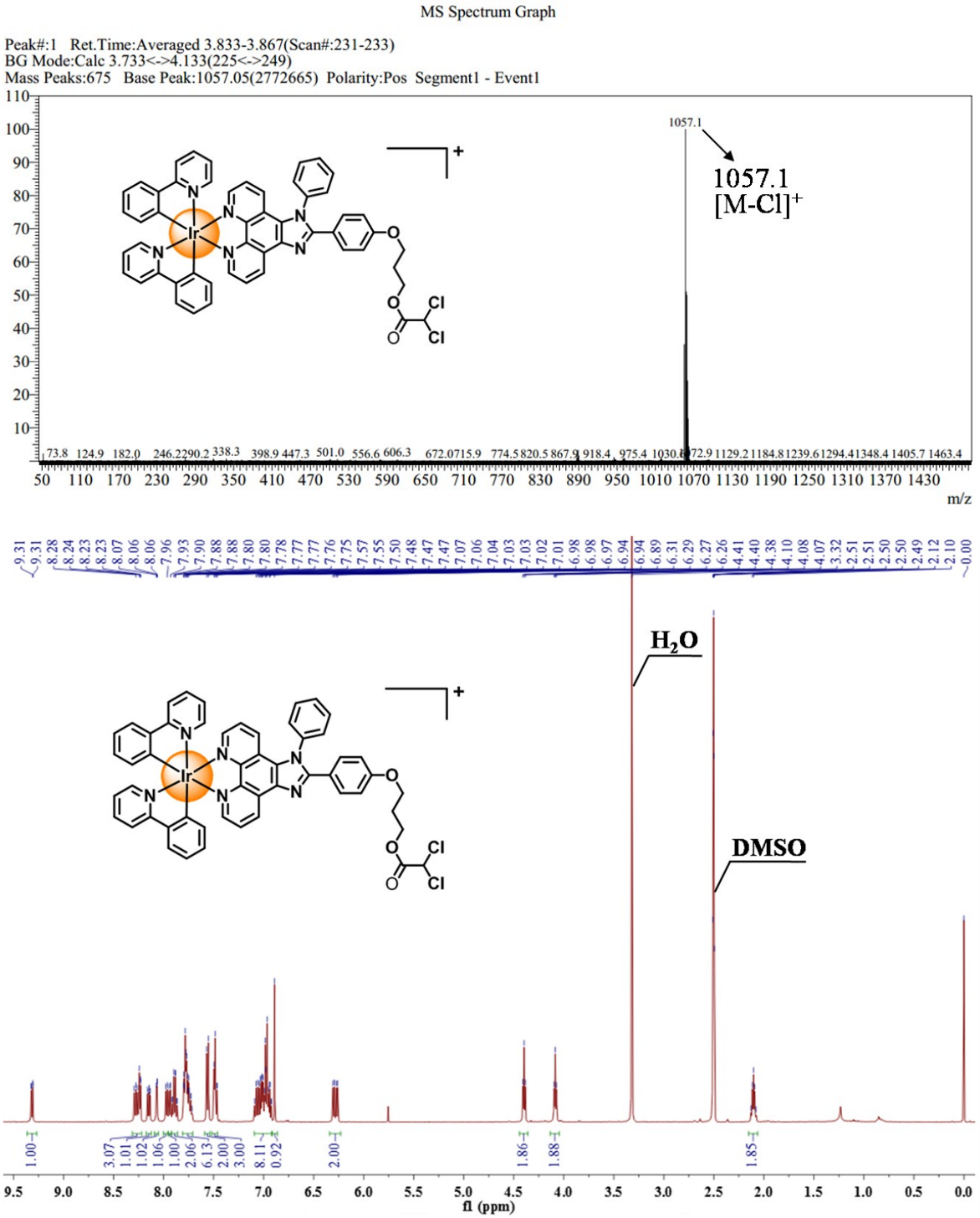

Figure S2. ESI-MS, and ^{1}H NMR spectrum of **Ir2**。

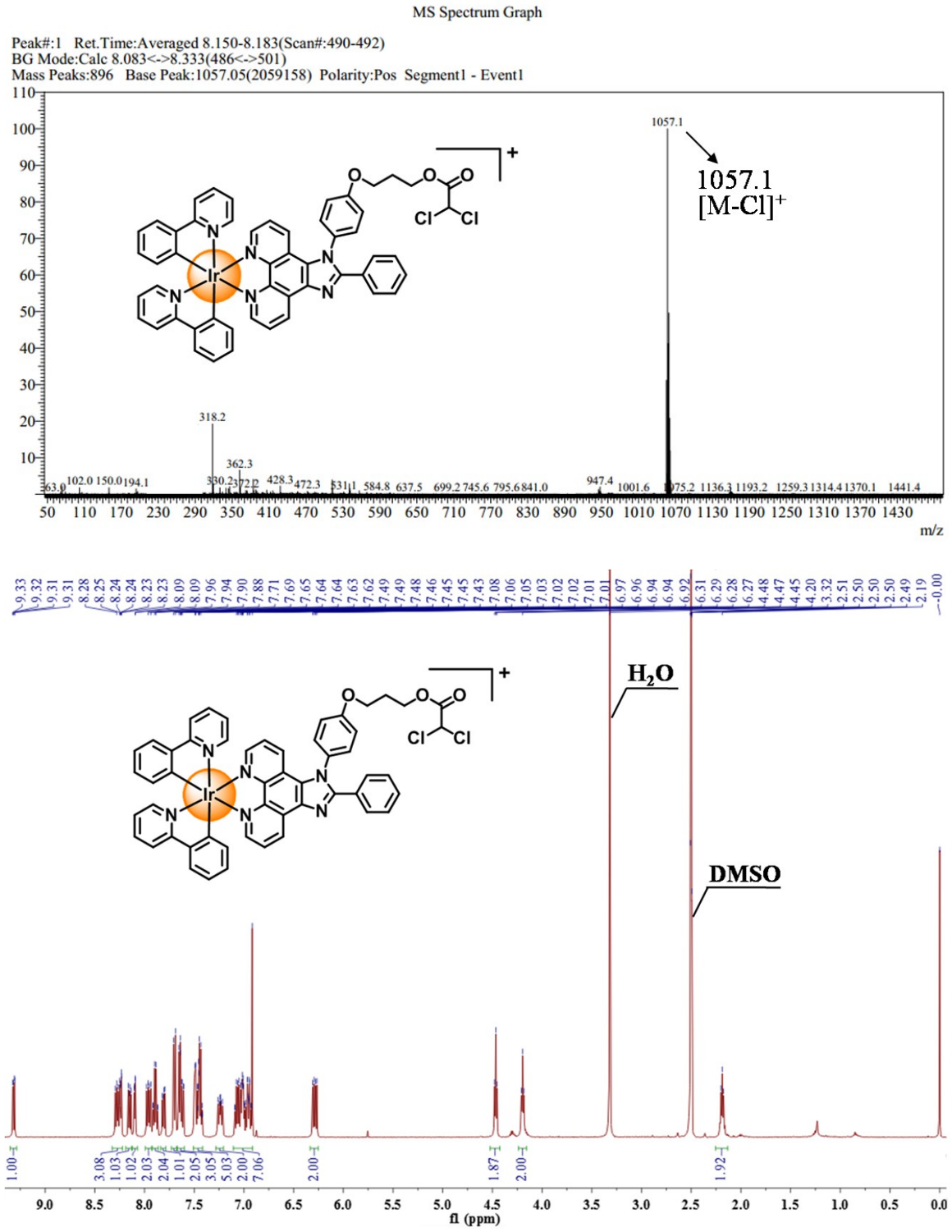

Figure S3. ESI-MS, and ^{1}H NMR spectrum of **Ir3**。

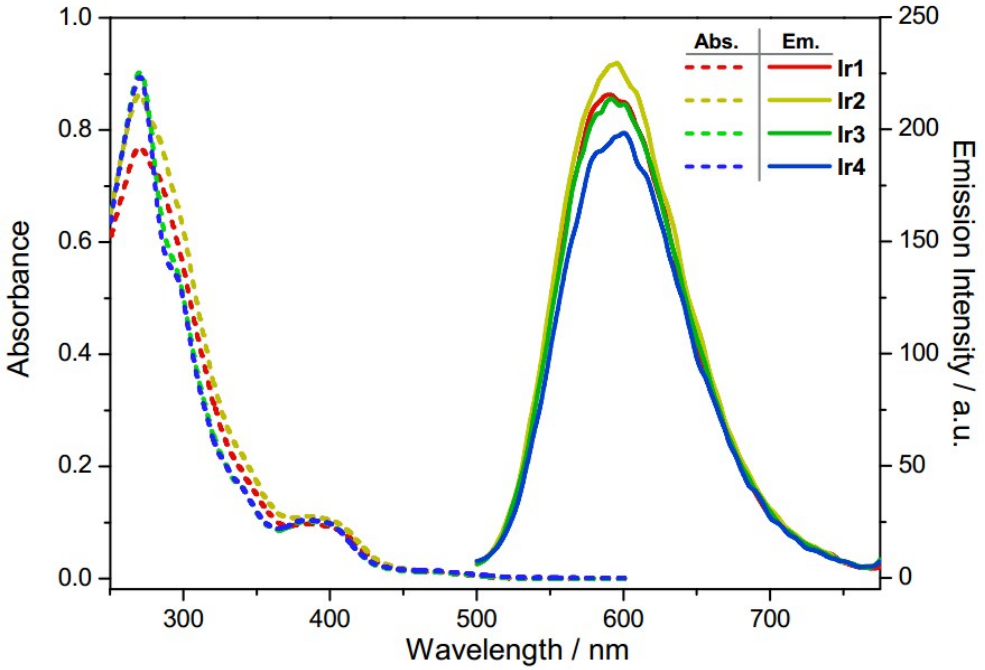

Figure S4. UV-vis absorption and emission spectra of **Ir1-Ir4** (10 μM) in MeOH solutions at room temperature under excitation of 365 nm xenon lamp.

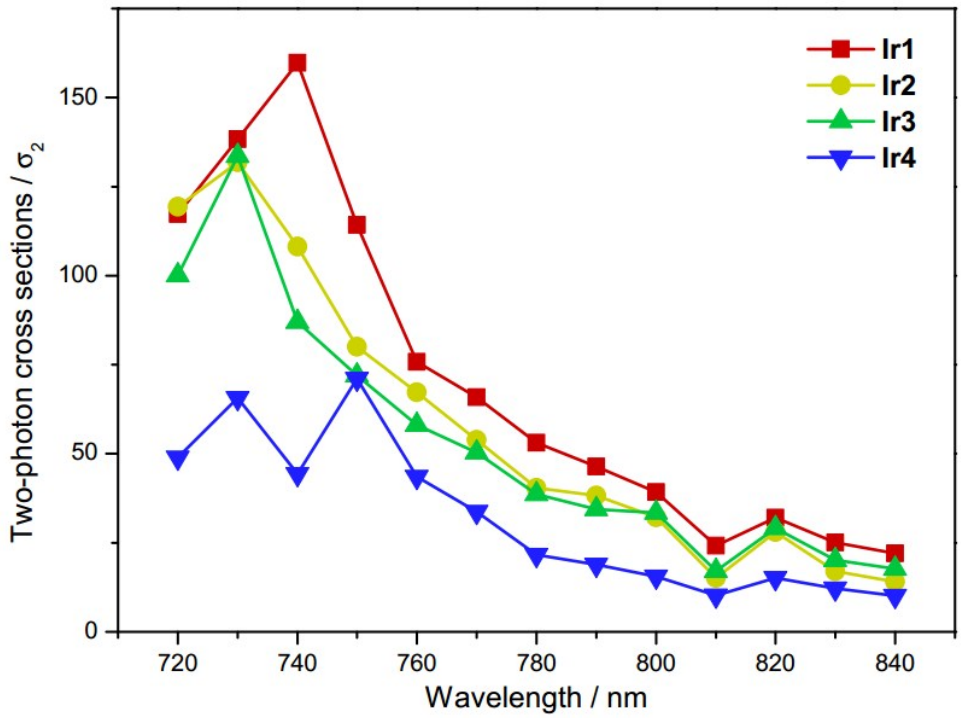

Figure S5. Two-photon cross sections of **Ir1-Ir4** at varying excitation wavelength ranging from 720 nm to 840 nm.

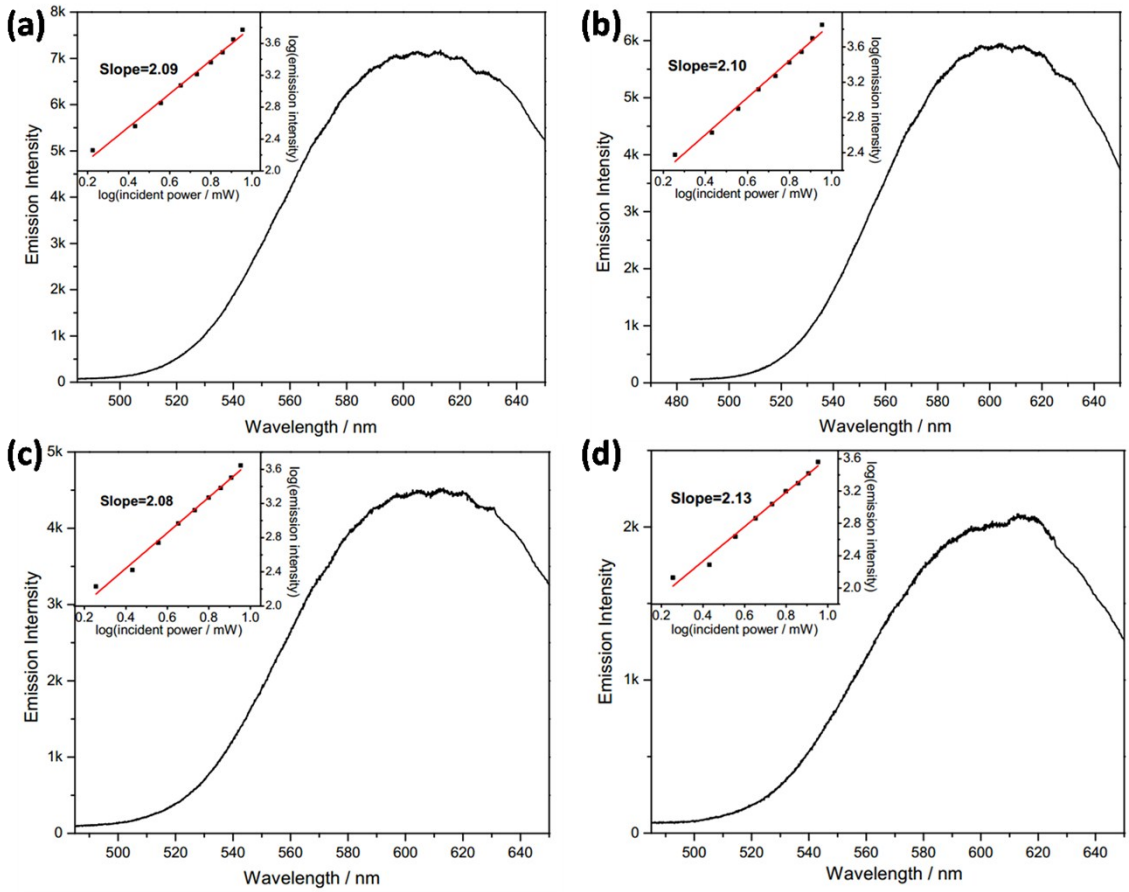

Figure S6. Two-photon induced emission spectra of **Ir1** (a), **Ir2** (b), **Ir3** (c) and **Ir4** (d). Inset: The logarithmic plots of the power dependence of relative two-photon induced luminescence intensity of the complexes as a function of pump power at the excitation wavelength corresponding to the maximal two-photon cross sections. The solid lines are the best-fit straight lines with gradient around 2.

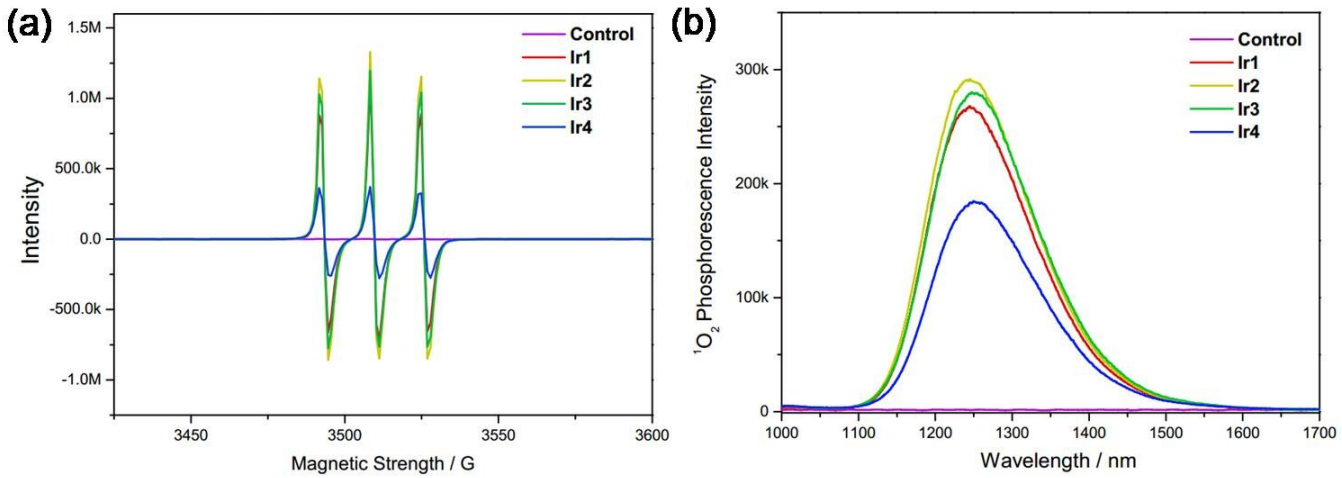

Figure S7. (a) TEMPO signal captured from air-saturated MeOH solution containing TEMP and Ir complexes (OD_{405} = 0.2, no Ir complexes were added in control) after irradiation (λ_{irr} = 405 ± 10 nm, 20 mW cm^{-2}, 5 min) in ESR; (b) The $^1O_2$ phosphorescence spectra of **Ir1-Ir4** (OD_{405} = 0.2) in $CDCl_3$ (λ_{irr} = 405 nm).

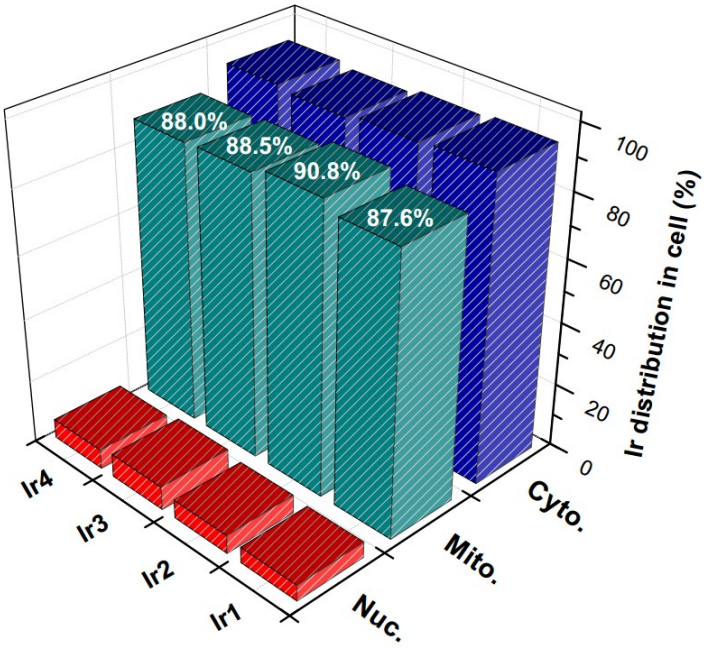

Figure S8. ICP-MS quantification of the internalized Ir by the HeLa cells. HeLa cells were treated with **Ir1-Ir4** (0.2 μM) at 37 C for 1 h in the dark. Nuclei (Nuc.), mitochondria (Mito.) and cytoplasm (including mitochondria) were extracted using mitochondrial and nuclear isolation kits.

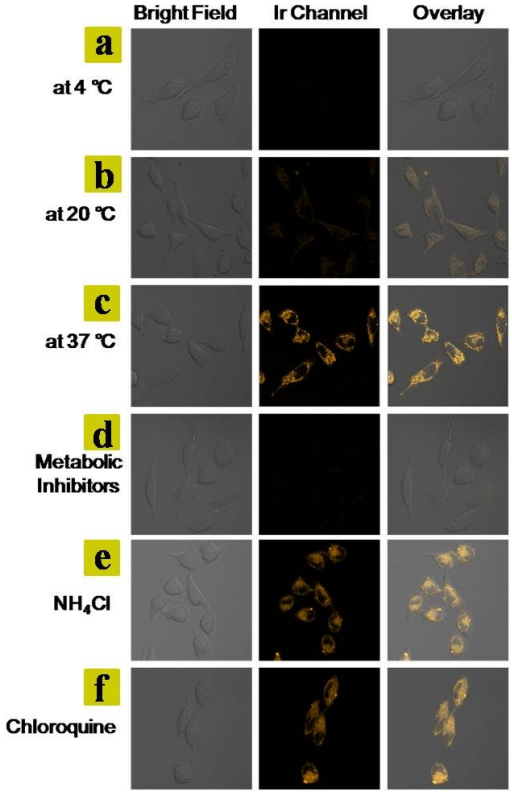

Figure S9. Confocal luminescence images and bright-field images of live HeLa cells preincubated with 0.2 μM **Ir1** for 30 min under different conditions. (a) The cells were incubated at 4 °C. (b) The cells were incubated at 20 °C. (c) The cells were incubated at 37 °C. (d) The cells were incubated with 50 mM 2-deoxy-D-glucose and 5 μM oligomycin for 1 h prior to the incubation of **Ir1**. (e) The cells were treated with 50 mM NH_4Cl for 1 h in advance and then incubated with **Ir1**. (f) The cells were pretreated with 50 μM Choroquine for 1 h before the incubation of **Ir1**.

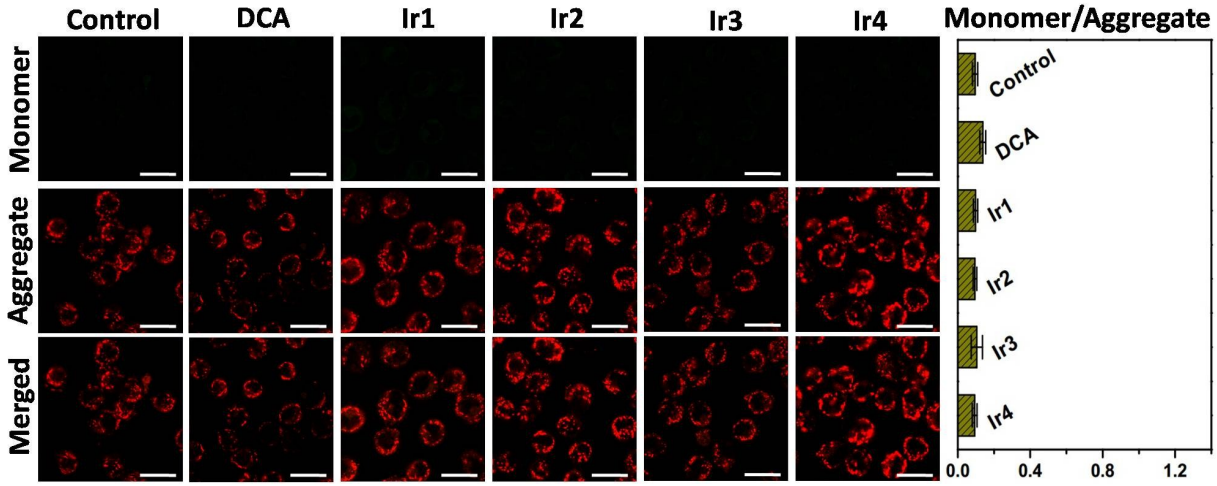

Figure S10. Effects of DCA (20 μM), **Ir1-Ir4** (0.5 μM) on mitochondrial membrane potentials of L02 cells after 6 h incubation in the dark.

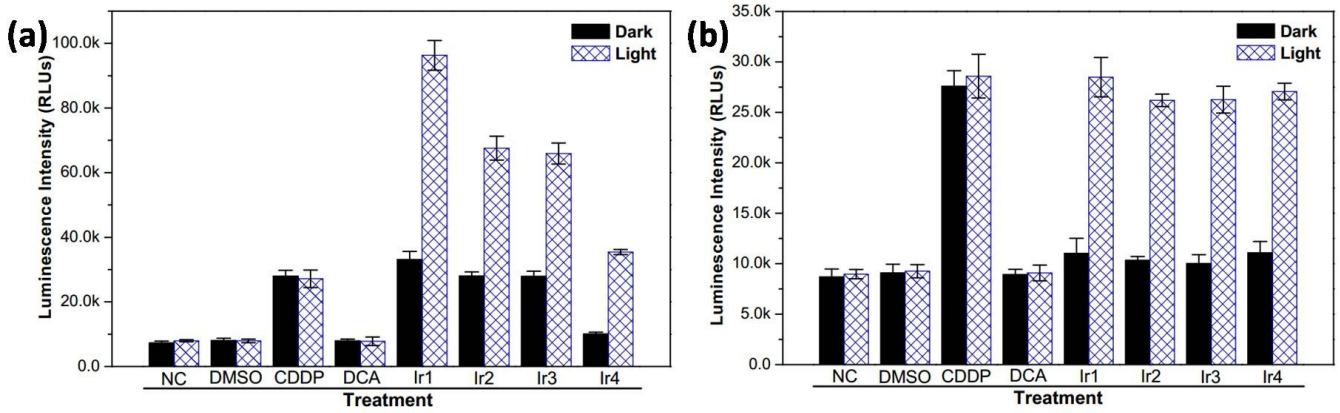

Figure S11. Activation of Caspase-3/7 in HeLa (a)/L02 (b) cells pre-treated with culture medium (negative control), DMSO (0.5%), 20 μM cisplatin (CDDP), 20 μM DCA, and 0.5 μM **Ir1-Ir4**, respectively, for 12 h with/without OPA-PDT treatment. The measurement was conducted 2 h after the irradiation.

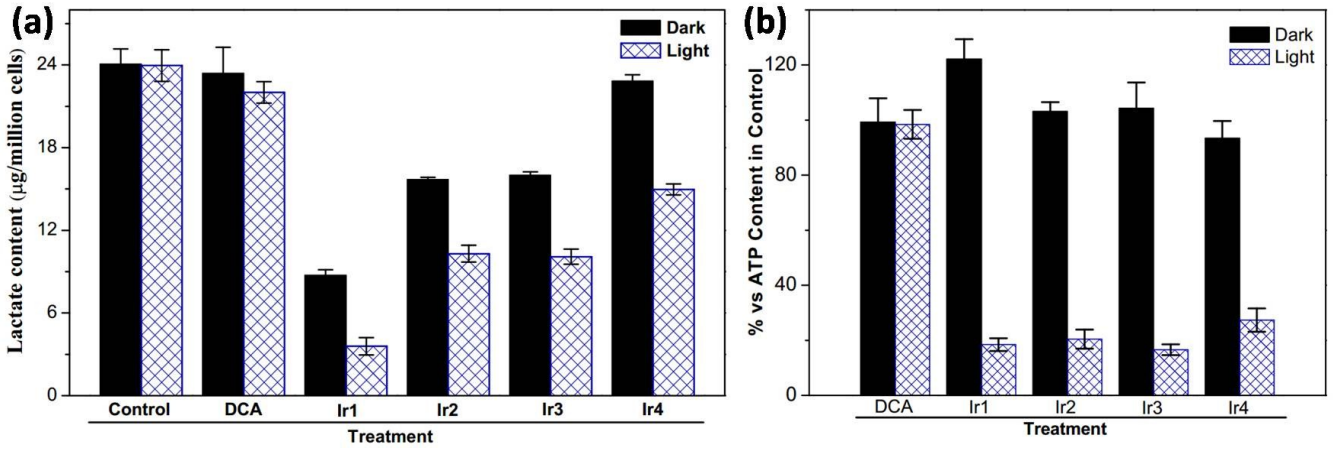

Figure S12. Lactate levels (a) and ATP levels (b) in HeLa cells treated with culture medium (control), 20 μM DCA, 0.5 μM **Ir1-Ir4** at 37 °C for 4 h with/without PDT treatment (405 ± 10 nm, 6 J cm^{-2}).

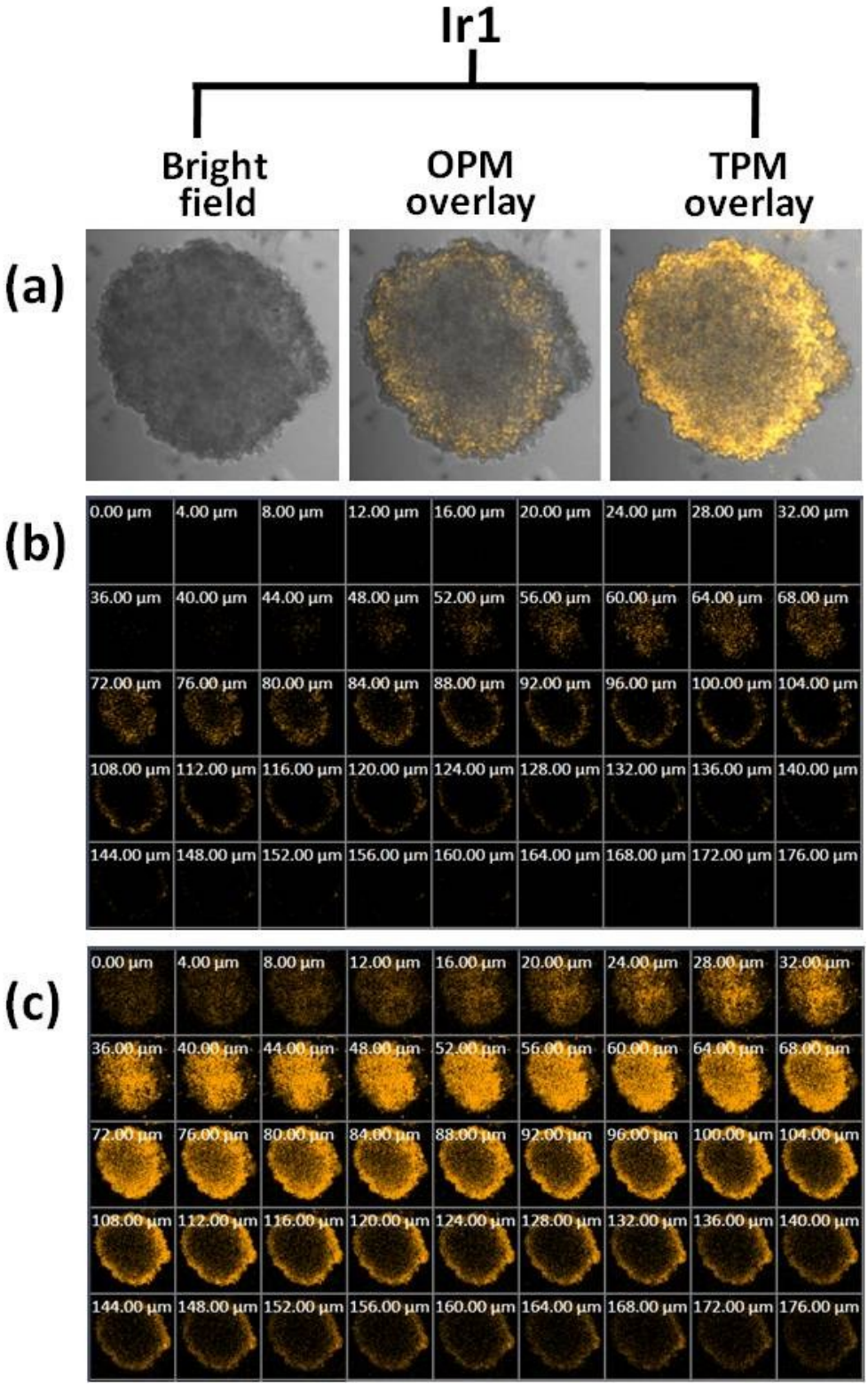
Ir1
Bright field
OPM overlay
TPM overlay
(a)
(b)
0.00 µm 4.00 µm 8.00 µm 12.00 µm 16.00 µm 20.00 µm 24.00 µm 28.00 µm 32.00 µm
36.00 µm 40.00 µm 44.00 µm 48.00 µm 52.00 µm 56.00 µm 60.00 µm 64.00 µm 68.00 µm
72.00 µm 76.00 µm 80.00 µm 84.00 µm 88.00 µm 92.00 µm 96.00 µm 100.00 µm 104.00 µm
108.00 µm 112.00 µm 116.00 µm 120.00 µm 124.00 µm 128.00 µm 132.00 µm 136.00 µm 140.00 µm
144.00 µm 148.00 µm 152.00 µm 156.00 µm 160.00 µm 164.00 µm 168.00 µm 172.00 µm 176.00 µm
(c)
0.00 µm 4.00 µm 8.00 µm 12.00 µm 16.00 µm 20.00 µm 24.00 µm 28.00 µm 32.00 µm
36.00 µm 40.00 µm 44.00 µm 48.00 µm 52.00 µm 56.00 µm 60.00 µm 64.00 µm 68.00 µm
72.00 µm 76.00 µm 80.00 µm 84.00 µm 88.00 µm 92.00 µm 96.00 µm 100.00 µm 104.00 µm
108.00 µm 112.00 µm 116.00 µm 120.00 µm 124.00 µm 128.00 µm 132.00 µm 136.00 µm 140.00 µm
144.00 µm 148.00 µm 152.00 µm 156.00 µm 160.00 µm 164.00 µm 168.00 µm 172.00 µm 176.00 µm

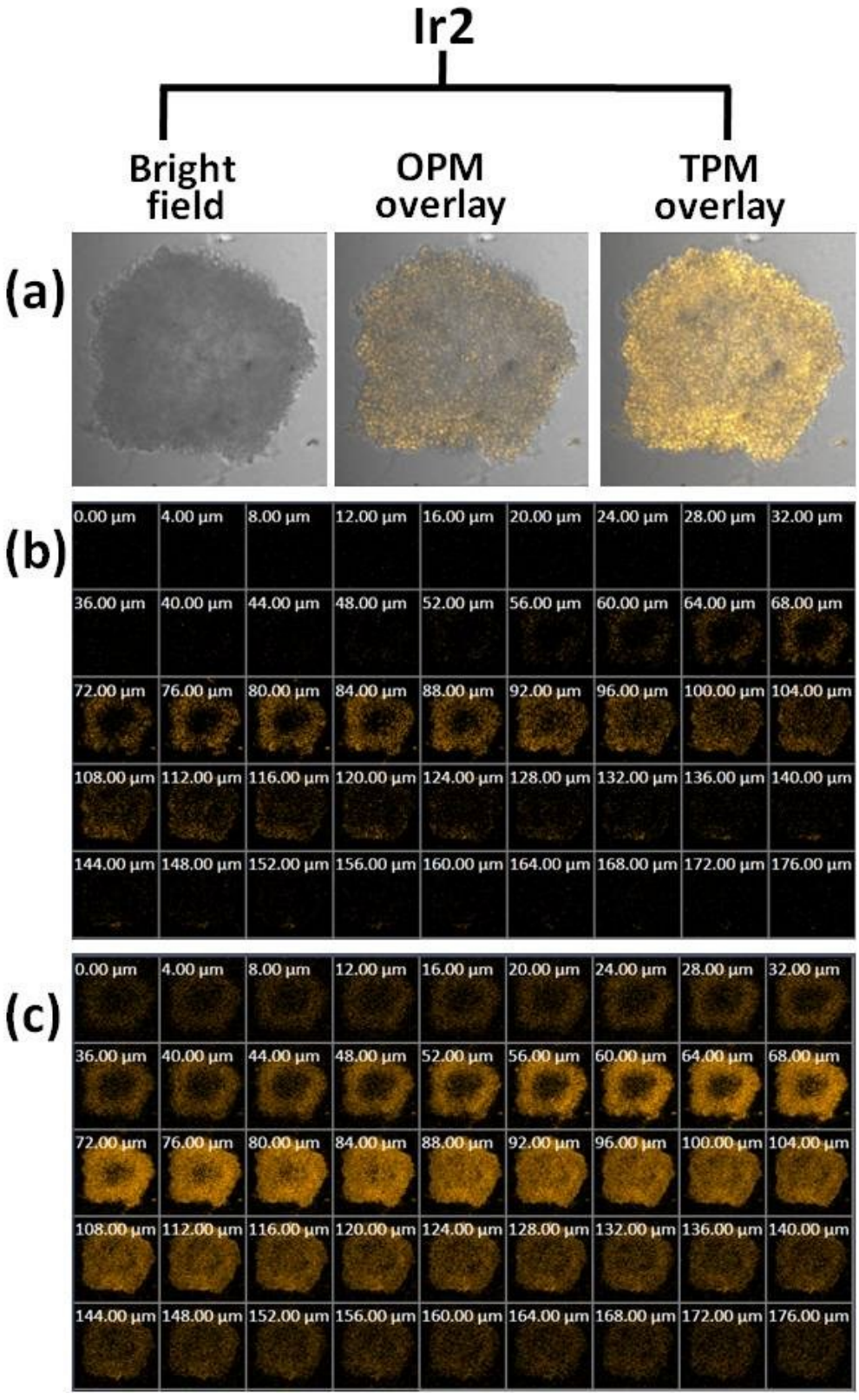
Ir2
Bright field
OPM overlay
TPM overlay
(a)
(b)
(c)
0.00 µm
4.00 µm
8.00 µm
12.00 µm
16.00 µm
20.00 µm
24.00 µm
28.00 µm
32.00 µm
36.00 µm
40.00 µm
44.00 µm
48.00 µm
52.00 µm
56.00 µm
60.00 µm
64.00 µm
68.00 µm
72.00 µm
76.00 µm
80.00 µm
84.00 µm
88.00 µm
92.00 µm
96.00 µm
100.00 µm
104.00 µm
108.00 µm
112.00 µm
116.00 µm
120.00 µm
124.00 µm
128.00 µm
132.00 µm
136.00 µm
140.00 µm
144.00 µm
148.00 µm
152.00 µm
156.00 µm
160.00 µm
164.00 µm
168.00 µm
172.00 µm
176.00 µm

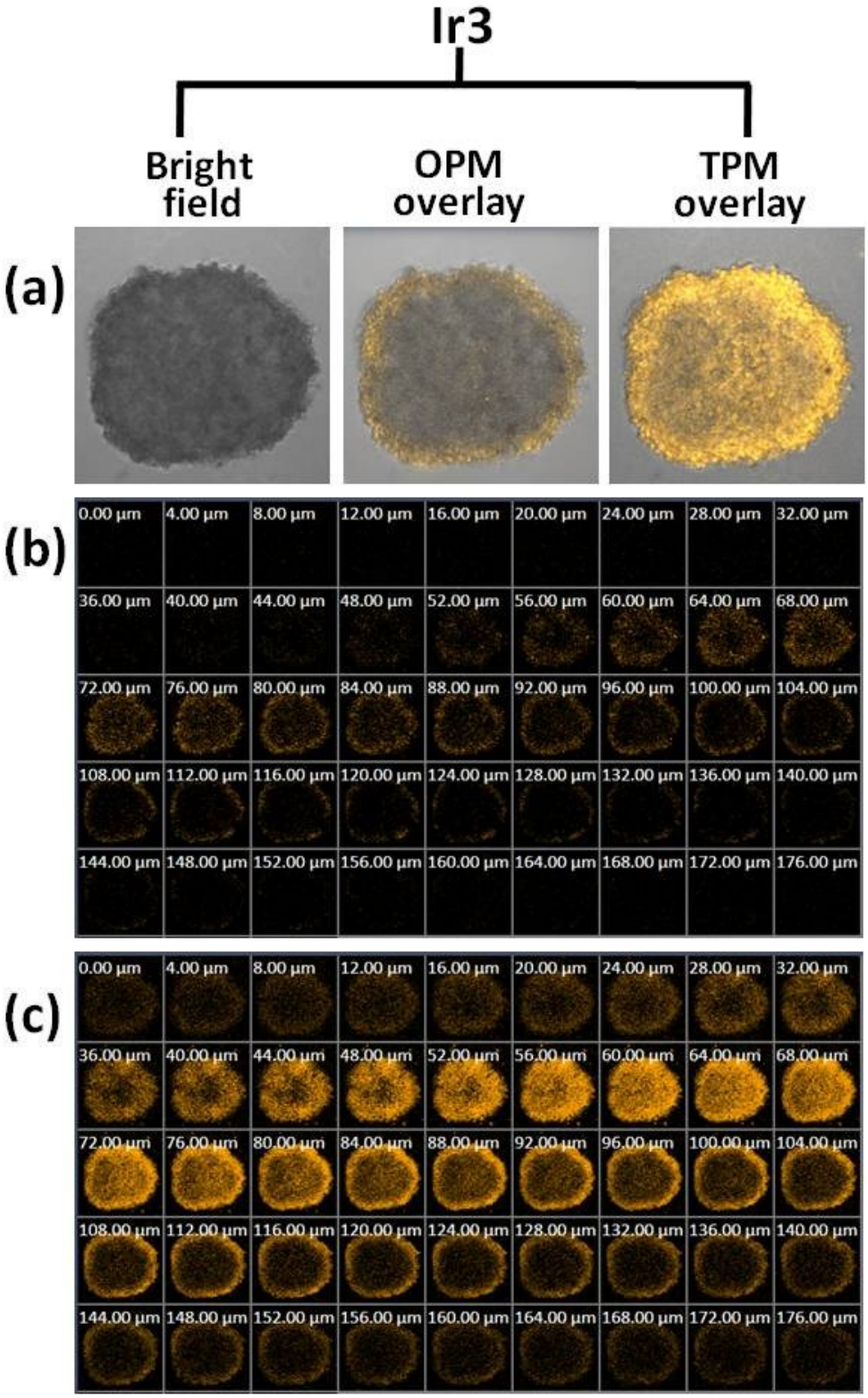
Ir3
Bright field
OPM overlay
TPM overlay
(a)
(b)
(c)
0.00 µm
4.00 µm
8.00 µm
12.00 µm
16.00 µm
20.00 µm
24.00 µm
28.00 µm
32.00 µm
36.00 µm
40.00 µm
44.00 µm
48.00 µm
52.00 µm
56.00 µm
60.00 µm
64.00 µm
68.00 µm
72.00 µm
76.00 µm
80.00 µm
84.00 µm
88.00 µm
92.00 µm
96.00 µm
100.00 µm
104.00 µm
108.00 µm
112.00 µm
116.00 µm
120.00 µm
124.00 µm
128.00 µm
132.00 µm
136.00 µm
140.00 µm
144.00 µm
148.00 µm
152.00 µm
156.00 µm
160.00 µm
164.00 µm
168.00 µm
172.00 µm
176.00 µm

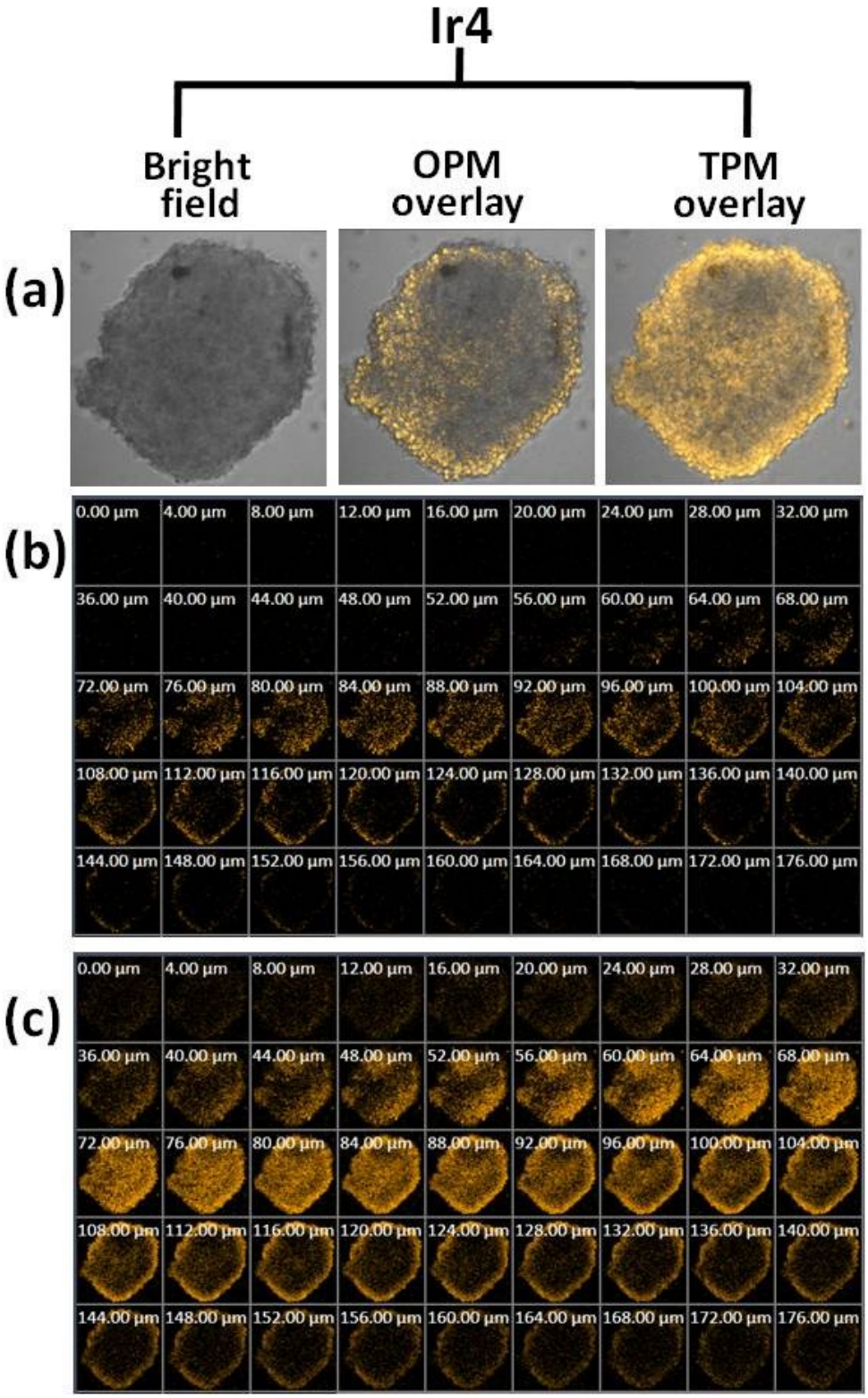

Figure S13. OPM and TPM Z-stack images of 3D HeLa MCSs after incubation with **Ir1-Ir4**, respectively for 2 h (concentration of 0.2 μM); a) From left to right: Brightfield, OPM overlay, TPM overlay; b) Substrate of OPM and TPM Z-axis scanning images captured from the top to the bottom of an intact 400 μm spheroid; c) The one-photon and two-photon 3D Z-stack images of an intact spheroid. The excitation wavelengths of OPM and TPM were 405 nm and 730 nm (**Ir2, Ir3**)/740 nm (**Ir1**)/750 nm (**Ir4**), respectively.

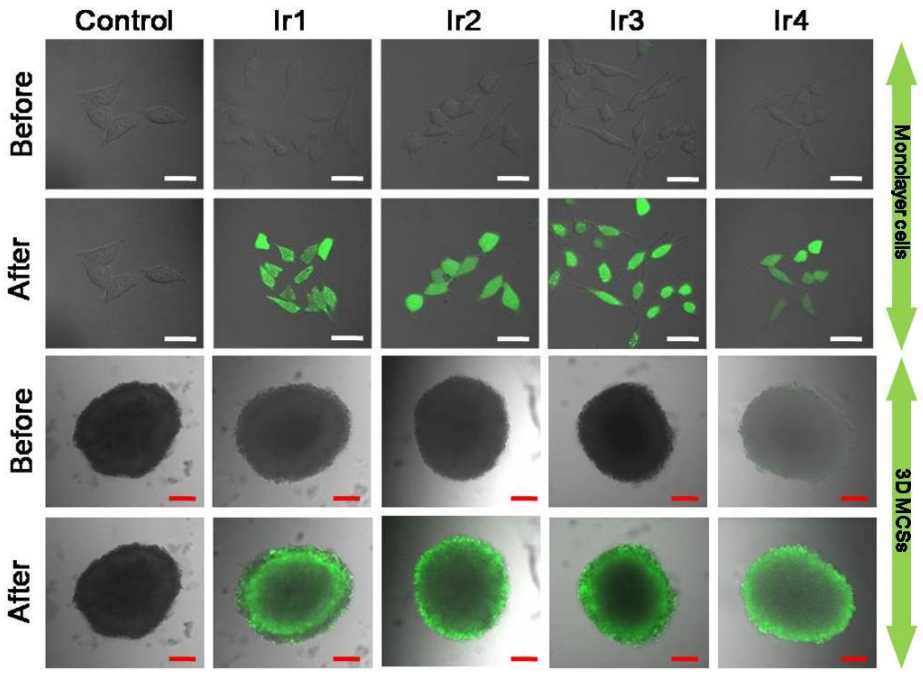

Figure S14. Confocal images of HeLa cells/MCSs before and after TP PDT. Cells were pre-incubated with DCFH-DA (λ_{em} = 510-550 nm, λ_{ex} = 488 nm) and **Ir1**-**Ir4** (0.5 μM), inset scale bar 20 μm (white)/100 μm (red).

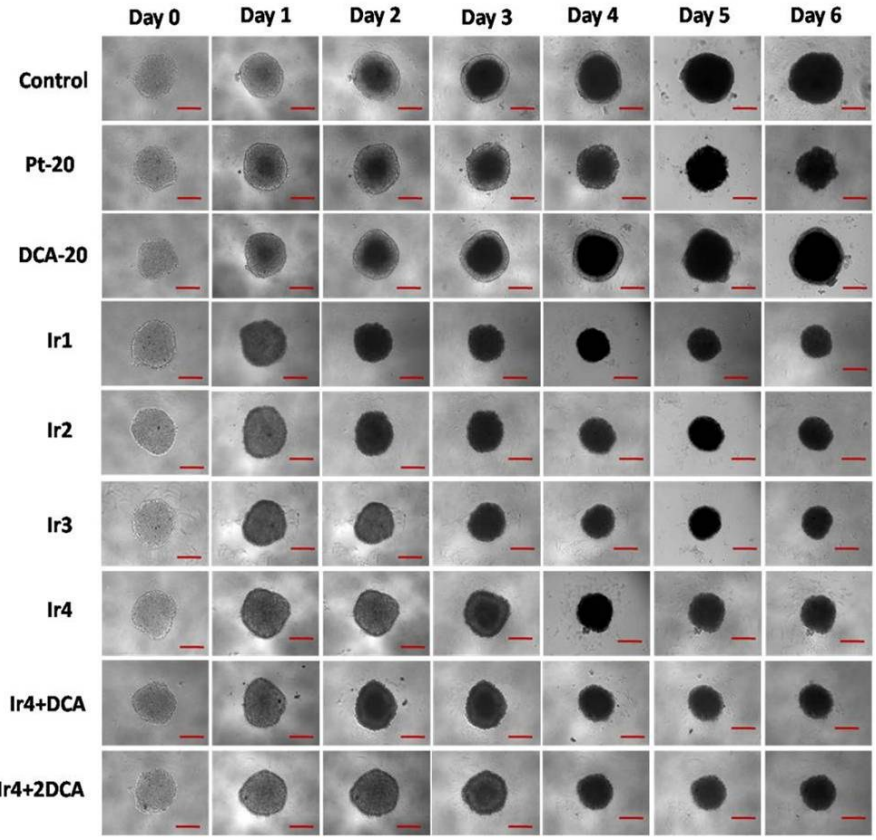

Figure S15. Representative images of MCSs treated DMEM (control), cisplatin (20 μM)，DCA (20 μM) and **Ir1–4** (0.5 μM), respectively, over 6 days. The MCSs were subjected to two-photon laser irradiation (1.2 W cm^{-2}, 1 kHz, 110 fs, 12 J cm^{-2} per section, section interval: 3 μm) at 730 nm (**Ir2, Ir3**)/740 nm (**Ir1**)/750 nm (**Ir4**), respectively on Day 3. The inset scale bar represents 200 μm.

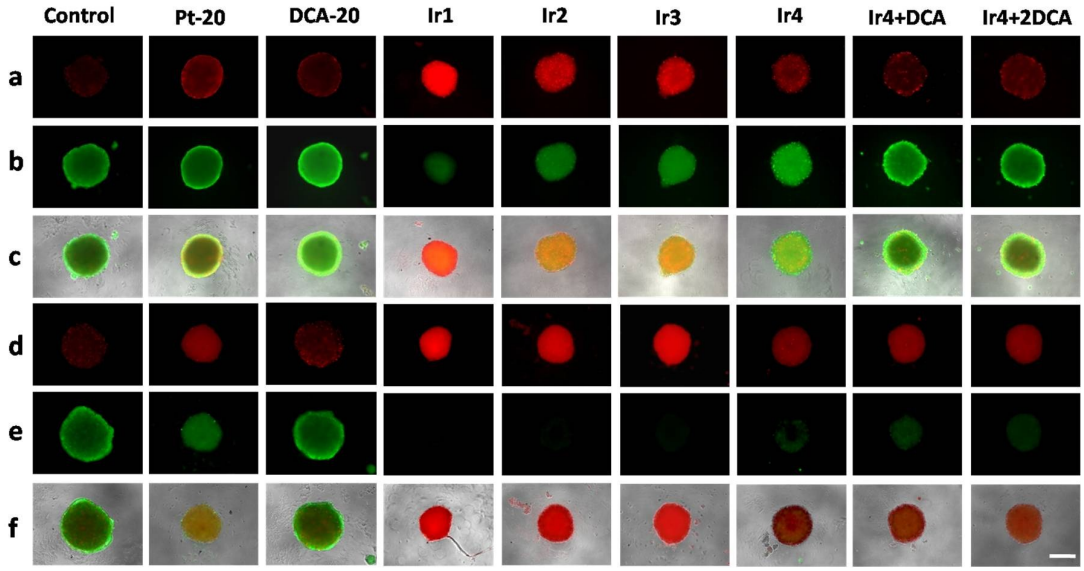

Figure S16. Representative images of calcein AM/EthD-1 co-staining on 3D HeLa MCSs after treatment with DMEM (control), cisplatin (20 μM), DCA (20 μM) and **Ir1-Ir4** (0.5 μM), respectively. a-c: 72 h after incubation in the dark (Day 3); d-f: incubated in the dark for 3 days, subjected to TP PDT (12 J cm^{-2}/section, section interval = 3 μm) and incubated for additional 48 h in the dark (day 5); a, d: Calcein AM channel; b, e: EthD-1 channel; c, f: Overlay of bright field and the dye channels. Inset scale bars denote 200 μm.

Table S1 Photophysical properties of **Ir1-Ir4**

Compd	λ_{abs}/ nm (log ε) [a]	λ_{em} / nm[b]	Φ_{PL}	τ / ns	σ_2[b]/GM	$\Phi_{PL} \times \sigma_2$[c]
Ir1	270(4.87), 386 (3.99)	590	0.061	185	159	9.7
Ir2	272(4.93), 384(4.05)	593	0.064	180	131	8.4
Ir3	270(4.96), 384(4.01)	591	0.063	183	133	8.4
Ir4	270(4.95), 384(4.02)	603	0.068	156	78.2	5.3

[a] Data were obtained in aerated MeOH and the exitation wavelength is 365 nm. [b] Maximum two-photon absorption cross section, σ_2, at 730 nm. [c] $\Phi_{PL} \times \sigma_2$ higher than the 0.1 GM threshold for optical imaging application in live specimens.

Table S2. Estimation of TPA-induced ROS generating ability.[a]

Compd	σ_2/GM	Φ_Δ	$\Phi_\Delta \times \sigma_2$
H_2TPP	2.2[b]	0.70[b]	1.5
Ir1	159	0.68	108
Ir2	131	0.74	97
Ir3	133	0.70	93
Ir4	78.2	0.53	41

[a] Data of **Ir1-Ir4** were collected in MeOH, data of H_2TPP were measured in toluene. [b] Value taken from reference[12]

.

Table S3. The content of Ir in 10^6 HeLa cells and their distribution in nuclei, cytoplasm and mitochondria.

Compd	Ir content (ng)			
	whole cell	Mitochondria	Nuclei	Cytoplasm (Without mitochondria)
Ir1	6.54 ± 0.45	5.73 ± 0.19	0.329 ± 0. 075	0.486 ± 0.010
Ir2	8.11 ± 0.55	7.36 ± 0.13	0.476 ± 0. 083	0.272 ± 0.016
Ir3	7.18 ± 0.44	6.35 ± 0.26	0.528 ± 0.045	0.296± 0.018
Ir4	4.22 ± 0.34	3.72 ± 0.26	0.257± 0.017	0.248± 0.014

Table S4 (Photo)cytotoxicity (IC_{50} [μM]) towards different cell lines in 2D model.[a]

Cell line	A549			A549R		
Treatment	dark	Light	PI	dark	light	PI
Cisplatin	9.9±1.8	10.4±0.8	0.95	35.5±3.2	36.5±3.1	0.97
H_2TPP	>100	89.1±3.8	nd	>100	89.4±4.8	nd
DCA	>100	>100	nd	>100	>100	nd
Ir1	2.10±0.11	0.36±0.11	5.8	2.73±0.10	0.41±0.10	6.7
Ir2	3.82±0.09	0.46±0.13	8.3	3.92±0.16	0.62±0.12	6.3
Ir3	3.92±0.21	0.52±0.02	7.5	3.95±0.08	0.61±0.11	6.4
Ir4	8.32±0.52	0.89±0.10	9.3	8.08±1.10	0.91±0.09	8.8
Ir4+DCA	8.57±0.20	0.88±0.10	9.9	8.12±0.80	0.95±0.05	8.5
Ir4+2DCA	8.66±0.87	0.87±0.09	9.9	8.14±0.60	0.91±0.16	8.9
Cell line	L02			HeLa		
Treatment	Dark	light	PI	dark	light	PI
Cisplatin	6.1±0.8	5.8±0.8	1.0	5.1±0.8	4.9±0.8	1.0
H_2TPP	>100	81.3±2.4	nd	>100	82.2±5.8	nd
DCA	>100	>100	nd	>100	>100	nd
Ir1	8.91±0.70	3.30±0.40	2.7	1.58±0.08	0.10±0.005	16
Ir2	9.02±1.10	3.11±0.80	2.9	2.52±0.11	0.21±0.06	12
Ir3	8.96±1.80	2.95±0.40	3.0	2.61±0.12	0.27±0.04	9.6
Ir4	9.40±1.40	3.52±0.60	2.7	7.77±0.20	0.94±0.15	8.2
Ir4+DCA	9.50±0.70	3.54±0.90	2.7	7.72±0.30	0.92±0.11	8.4
Ir4+2DCA	9.33±1.90	3.55±0.20	2.6	7.83±0.40	0.95±0.09	8.2

[a] Irradiated at 450 nm by an LED area light (405 ± 10 nm, 20 mW cm^{-2}, light dose = 6 J cm^{-2}).

Table S5 (Photo)cytotoxicity (IC_{50} [μM]) towards 400 μm 3D HeLa MCSs.

Compound	Dark	OPA[a]	PI	TPA[b]	PI
Cisplatin	12.8±2.3	12.6±1.9	1.0	12.2±1.7	1.0
H_2TPP	> 100	> 100	nd	> 100	nd
DCA	> 100	> 100	nd	> 100	nd
Ir1	1.92±0.10	0.15±0.04	7.9	0.11±0.03	16
Ir2	3.08±0.12	0.44±0.12	7.0	0.38±0.13	8.1
Ir3	3.17±0.07	0.42±0.09	7.5	0.37±0.10	8.6
Ir4	11.2±1.10	2.32±0.14	4.8	2.57±0.29	4.5
Ir4+DCA	11.0±0.81	2.38±0.19	4.6	2.54±0.24	4.7
Ir4+2DCA	10.9±0.95	2.32±0.17	4.6	2.51±0.22	4.5

[a] Irradiated at 405 nm by an LED area light (405 ± 10 nm, 20 mW cm^{-2}, light dose = 6 J cm^{-2}). [b] Irradiated at 730-750 nm using a confocal microscope equipped with a mode-locked Ti:sapphire laser source (1.2 W cm^{-2}, 1kHz, pulse width 110 fs, light dose = 12 J cm^{-2}/section, section interval = 3 μm, scanned area for each section was *ca.* 1.5 × 1.5 mm). Data shown are values from three replicates.

Reference

1 (a) G. A. Crosby, J. N. Demas, *J. Phys. Chem.,* 1971, **75**, 991-1024; (b) J. V. Caspar, T. J. Meyer, *J. Am. Chem. Soc.,* 1983, **105**, 5583-5590.

2 J. Liu, Y. Chen, G. Li, P. Zhang, C. Jin, L. Zeng, L. Ji, H. Chao, *Biomaterials,* 2015, **56**, 140-153.

3 C. Jin, J. Liu, Y. Chen, L. Zeng, R. Guan, C. Ouyang, L. Ji, H. Chao, *Chem. Eur. J.,* 2015, **21**, 12000-12010.

4 C. Xu, W. W. Webb, *J. Opt. Soc. Am. B.,* 1996, **13**, 481-491.

5 N. S. Makarov, M. Drobizhev, A. Rebane, *Opt. Exp.,* 2008, **16**, 4029-4047.

6 W. Adam, D. V. Kazakov, V. P. Kazakov, *Chem. Rev.,* 2005, **105**, 3371-3387.

7 A. A. Abdel-Shafi, P. D. Beer, R. J. Mortimer, F. Wilkinson, *J. Phys. Chem. A.,* 1999, **104**, 192-202.

8 H.-Y. Ding, X.-S. Wang, L.-Q. Song, J.-R. Chen, J.-H. Yu, L. Chao, B.-W. Zhang, *J. Photochem. Photobiol. A.,* 2006, **177**, 286-294.

9 C. Li, M. Yu, Y. Sun, Y. Wu, C. Huang, F. Li, *J. Am. Chem. Soc.,* 2011, **133**, 11231-11239.

10 H. Huang, P. Zhang, B. Yu, Y. Chen, J. Wang, L. Ji, H. Chao, *J. Med. Chem.,* 2014, **57**, 8971-8983.

11 A. Gomes, E. Fernandes, J. L. Lima, *J. biochem. biophys. meth.,* 2005, **65**, 45-80.

12 T. Ishi-i, Y. Taguri, S.-i. Kato, M. Shigeiwa, H. Gorohmaru, S. Maeda, S. Mataka, *J. Mater. Chem.,* 2007, **17**, 3341-3346.